

**FORMATION OF TOMA HILLS IN THE AREA OF THE
FERNPASS ROCKSLIDE IN TYROL, AUSTRIA**

by

KAGISO SAMUEL MORE

Submitted in partial fulfilment of the requirements for the
degree

MAGISTER TECHNOLOGIAE: GEOLOGY

in the

Department of Environmental, Water and Earth Sciences

FACULTY OF SCIENCE

TSHWANE UNIVERSITY OF TECHNOLOGY

Supervisor: Prof. Dr habil. Ch. Wolkersdorfer

Co-Supervisor: Dr M Lupankwa

September 2018

Declaration

I hereby declare that the dissertation submitted for the degree M. Tech: Geology, at Tshwane University of Technology, is my own original work and has not previously been submitted to any other institution of higher education. I further declare that all sources cited or quoted are indicated and acknowledged by means of a comprehensive list of references.

Kagiso Samuel More

Copyright© Tshwane University of Technology 2018

Acknowledgements

I would like to express my sincere gratitude to my supervisor, Prof C Wolkersdorfer and co-supervisor, Dr M Lupankwa, for the continuous support of my master's study, for their patience, motivation and immense knowledge. Their guidance helped in all the time of research and writing of this dissertation. I could not have imagined having better supervisors for my master's study.

Besides my supervisors, I would like to thank my friends and family for their insightful comments and encouragement, the institution, Tshwane University of Technology, for allowing me to use their laboratory facilities to conduct my research.

Financial assistance provided by the National Research Foundation (NRF) South Africa under the SARChI Chair for Mine Water Management in respect of the costs of this study is hereby acknowledged.

Presentations and Publications

The work contained in this thesis has previously been presented at conferences and published in Journal Articles as indicated below.

Conference presentation

Wolkersdorfer C., More K. & Lupankwa M. Analoge Modellierung von Tomahügeln [An Analogue Toma Hill Model]. Oral presentation. Geoforum Umhausen, 17-23 October 2017, Umhausen, Tyrol, Austria.

Publications

Wolkersdorfer, C., More, K. & Lupankwa, M. 2017. Analoge Modellierung von Tomahügeln [An analogue Toma Hill Model], In: Heißel, G., Mostler, W. (Eds.), Geoforum Umhausen, Umhausen, pp. 61-69.

Submitted: Kagiso S. More & Christian Wolkersdorfer. 2019. An Analogue Toma Hill Formation Model for the Tyrolian Fernpass Rockslide. Landslides. Springer, Berlin Heidelberg.

Abstract

The Fernpass rockslide occurred approximately 4100 years ago and is one of the largest of its kind in the Alps with a hummocky morphology and characteristic Toma Hills. Four hypotheses exist for their formation, and none of these can clarify all the features observed on site. To investigate a new hypothesis, a laboratory scale analogue groundwater flow model was used to examine the contribution of internal erosion by suffosion to forming Toma Hills.

A PVC tank measuring $1.5 \times 1.0 \times 0.8$ m with nine water inlets and three outlets was filled with synthetic rockslide material. Based on 45 existing sieve analyses of rockslide sediments, the synthetic rockslide material was developed. From the median values of the sieve analyses, hydraulic conductivities were calculated using the equations of Seelheim and Bialas. A total of five experiments, which ran for ± 30 days were performed by pumping tap water through the tank. Parameters such as flow, hydraulic gradient and compaction of the material were varied during each experiment. Eroded finer material and samples of the sediment after each experiment were taken for analysis by laser diffraction and sieve analysis. During the experiment all changes in morphology were recorded and videotaped.

The average hydraulic gradient of the experiments was set to be 2 times higher than that in reality. Hydraulic conductivities in the five experiments were comparable to the calculated field hydraulic conductivity (Bialas and Seelheim equations). A limnokrene similar to one south-west of Biberwier developed in all experiments. Development of

lateral and transversal cracks, water filled lateral depressions of the material in the model and discharge of finer material implicated that internal erosion is a substantial contribution to the Toma Hill formation.

Contents

Declaration.....	i
Acknowledgements.....	ii
Presentations and Publications.....	ii
Conference presentation	ii
Publications	ii
Abstract.....	iii
List of figures.....	vi
List of tables.....	ix
CHAPTER 1.....	1
1 Introduction.....	1
1.1 Brief summation of the dissertation	1
1.2 Background of the study.....	2
1.3 Problem statement and definitions	4
1.4 The Fernpass rockslide and Toma hills.....	7
1.5 Hypothesis.....	9
1.6 How can all of the Toma hills features be explained with the current knowledge...	10
1.7 Objectives of the study	11
CHAPTER 2.....	12
2 Site Description.....	12

2.1	Regional geology.....	12
2.2	Structural geology.....	12
2.3	Climate and vegetation.....	13
CHAPTER 3.....		14
3	Literature Study	14
3.1	Rockslide movement and factors influencing the occurrence of a rockslide	14
3.2	Other Alps rockslides associated with Toma hills.....	19
3.2.1	Flims rockslide (Switzerland).....	20
3.2.2	Tschirgant rockslide (Austria).....	22
3.2.3	Köfels rockslide (Austria).....	23
3.2.4	Sierre rockslide (Switzerland).....	24
3.2.5	Obernberg rockslide (Austria)	26
3.3	Previously proposed hypotheses for the formation of Toma hills	28
3.3.1	Karstification resulting in the formation of Toma hills	28
3.3.2	Transportation of rockslide material on a still existing glacier	29
3.3.3	Formation of Toma hills due to dead ice melting.....	30
3.3.4	Transportation of rockslide material on fluvial sediments.....	30
CHAPTER 4.....		32
4	Methods and Materials	32
4.1	Experimental design: Analogue model	32
4.2	Material selection and properties.....	33
4.3	Additional experimental procedures	38
CHAPTER 5.....		41

5	Results and Discussions.....	41
5.1	General features observed during the experiments	41
5.2	Discussion	49
5.3	Description of the eroded and lateral depression of material	53
5.4	Sieve analysis and laser diffraction	55
5.5	Tracer test	57
CHAPTER 6.....		60
6	Conclusion and Recommendations	60
CHAPTER 7.....		63
7	References	63

List of figures

Figure 1.1:	Overview of the study area. The Fernpass rockslide is slightly left of the centre of the map (© Google Earth, Wikipedia)	4
Figure 1.2:	The Fernpass rockslide internal structure (photographer: K.S. More).....	6
Figure 1.3:	Overview of the Fernpass rockslide near Biberwier (in the left of the image). 1: rockslide source area, 2: Fernpass lakes, 3: northern branch of the rockslide with 4: selected Toma Hills. Direction of view to the south-west (photographer: Ch. Wolkersdorfer).....	8
Figure 1.4:	Schematic cross section in the Fernpass rockslide area	9
Figure 1.5:	Conceptual model of the processes involved in Toma hill formation. Not to scale.	10
Figure 3.1:	Diagenetic features associated with carbonate-lithic rockslide deposits. Not to scale (after Sanders <i>et al.</i> , 2010).....	17
Figure 3.2:	Rockslide debris movement illustrated in three stages. Not to scale.....	18

Figure 3.3: Rockslide sediments in the Fernpass rockslide valley. The size of the book is 22 × 15 cm (photographer: K.S. More)	19
Figure 3.4: Conceptual drawing and cross section of the Tschirgant ridge on the left side and the shape of the Tschirgant rockslide on the right side. Not to scale.....	23
Figure 3.5: Overview of the Sierre rockslide (© Google Earth).....	26
Figure 3.6: Obernberg rockslide location (© Google Earth).....	26
Figure 3.7: Movement of the Obernberg deposits. Not to scale.	27
Figure 3.8: Schematic illustration of Sturzstrom supported by moving glacier. Not to scale.	29
Figure 3.9: Schematic illustration of how rockslide debris mix with and trail on fluvial sediments to form Toma hills. Not to scale.	31
Figure 4.1: Full view of the analogue model. A: showing the upper view and the inside of the tank on which outlets and inlets are seen from the inside covered with sieve, B: tank filled with material, C: showing the pumps used during the experiments, D: showing the outlets from the outer part of the tank, labelled O ₁ to O ₃ , E: inlets from the outer part of the tank, labelled I ₁ to I ₉ . Spacing of the marks 10 cm	34
Figure 4.2: Curves for the 45 sieve analyses in Schuch (1981). Green: moraine material, red: fluvial/glaciofluvial sediments and blue: rockslide debris.	35
Figure 4.3: The Hjulström diagram modified after Hjulström (1935) and Sundborg (1956) ..	40
Figure 5.1: A schematic sketch of the features observed during experiment № 1. Centimeter labels inside indicates the width of the cracks developed during the experiment. Also see electronic attachment A using the link www.wolkersdorfer.info/rockslide_more_A	42
Figure 5.2: Before (left) and after (right) the run of experiment № 1.....	43
Figure 5.3: A schematic sketch of the features observed during experiment № 2. Centimeter labels inside indicates the width of the cracks developed during the experiment. Also see electronic attachment B using the link www.wolkersdorfer.info/rockslide_more_B	44
Figure 5.4: Before (left) and after (right) the run of experiment № 2.....	44

Figure 5.5: A schematic sketch of the features observed during experiment № 3. Centimeter labels inside indicates the width of the cracks developed during the experiment. Also see electronic attachment C using the link www.wolkersdorfer.info/rockslide_more_C	45
Figure 5.6: Before (left) and after (right) the run of experiment № 3.....	46
Figure 5.7: A schematic sketch of the features observed during experiment № 4. Centimeter labels inside indicates the width of the cracks developed during the experiment. Also see electronic attachment D using the link www.wolkersdorfer.info/rockslide_more_D	47
Figure 5.8: Before (left) and after (right) the run of experiment № 4.....	47
Figure 5.9: A schematic sketch of the features observed during experiment № 5B. Centimeter labels inside indicates the width of the cracks developed during the experiment. Also see electronic attachment E using the link www.wolkersdorfer.info/rockslide_more_E	48
Figure 5.10: Before (left) and after (right) the run of experiment № 5B	49
Figure 5.11: Beginning of the formation of cracks and a water-filled depression during experiment № 1. Spacing of the marks 10 cm (photographer: More KS)	51
Figure 5.12: Formation of isolated Hills as cracks crossed during experiment № 5. Spacing of the marks 10 cm	52
Figure 5.13: Development of limnokrene; A: limnokrene developing during experiment № 3 (photographer: Ch. Wolkersdorfer), B: limnokrene at the Fernpass near Biberwier. Width of image is 2 m (photographer: K.S. More).....	53
Figure 5.14: The process of suffusion; i) intact material, ii) internal erosion taking place, iii) material after full internal erosion occurred	54
Figure 5.15: Development of lateral depression during experiment № 1. Spacing of the marks 10 cm (photographer: K.S. More).....	54
Figure 5.16: Experiments № 3 & 5 gradation curves of the sediments.....	56
Figure 5.17: Laser diffraction results for the limnokrene material near Biberwier and experiments № 4 and 5B eroded finer material	57
Figure 5.18: Tracer test setup during experiment № 5B, probes in the beakers placed adjacent to the outlets to measure the electrical conductivity	58

Figure 5.19: EC measurement during tracer test in experiment № 5B. A: indicates probe A measuring EC in outlet O₂, and B: indicates probe B measuring EC in outlet O₃. Peak at between 14:00 and 16:00 on the second day due to emptying the 60 L receiving container 59

List of tables

Table 3.1: Ages for the Tschirgant rockslide from different investigations and methods	22
Table 3.2: Ages for the Köfels rockslide from different methods.	24
Table 3.3: Age of the Sierre rockslide from ¹⁴ C-dating.....	25
Table 4.1: Statistical data of the 45 sieve analyses in Schuch (1981). Std. Dev.: Standard deviation of the population	35
Table 4.2: Calculated sediment mass based on the Schuch (1981) data, and real composition of the synthetic rock material used for experiments № 3 and 5. No results are available for experiments № 1, 2 and 4	36
Table 4.3: Summary of experiments № 1 to 5	37
Table 5.1: Mass of the eroded material of the experiments. Experiment 5A was stopped after some days, as material delivered had a too small grain size.....	50
Table 5.2: The hydraulic conductivity for the material on the northern branch determined by different methods	50
Table 5.3: Summary of sedimentological parameters of the Biberwier limnokrene material, and eroded finer material of experiments № 4 and 5B; C _u : uniformity coefficient, C _c : coefficient of curvature	56

CHAPTER 1

1 Introduction

1.1 Brief summation of the dissertation

The dissertation has been organised into six different sections, each with detailed information, and a number of annexures. A summation of each section is presented below:

Introduction

This section displays a general background on the Fernpass rockslide and Toma Hills. The aims and objectives of this study are briefly outlined in this section. A brief problem statement and hypothesis outline is also given.

Site Description

This section gives a clear overview on the regional geology, structural geology and depositional environment based on the literature review, hydrogeological investigations and field mapping of the study area. The geological group in which the rock types in this area are found is also presented in this section.

Literature Study

This section provides literature review on rockslides, explanation of types of movement, triggering mechanism and classification systems. A lot of the Alp's rockslides are characterised by Toma Hills and these rockslides are explained in this section. The previous proposed hypotheses for the formation of Toma Hills are also discussed.

Methods and Materials

This section summarises the methods used in this study, i.e. the construction of the analogue model as well as the material used. Laboratory procedures and tests are also discussed.

Results and Discussion

This part closes the loop of the main research aim which was to “investigate the potential contribution of internal erosion by suffosion in the formation of Toma Hills”. The results of the laboratory work, i.e. features observed during the experiments, particle size distribution and tracer test are explained in details in this section. Electronic attachment of all the raw data is available and can be accessed at www.wolkersdorfer.info/more_2018_data.

Conclusions and Recommendations

The discoveries of the investigation are outlined, and recommendations are put forward for further studies relating to this research study.

1.2 Background of the study

The downward mass movement of large, dry and loose material is a typical erosional process in mountainous areas as the Alps (Abele, 1974; Ampferer, 1904; Baltzer, 1874/75; Heim, 1932). Such occasions are frequently alluded to as dry rockslides (rock slide), rockfalls (rock falls) or rock topples (Erismann *et al.*, 2013; Imre *et al.*, 2010; Sassa *et al.*, 2007). The Alps are the setting for several small and large rockslides, and the rockslide occurrence in this region has attracted a wide research attention focusing on the causes of the rockslides, triggering mechanisms, climatic influences and the formation of Toma Hills (e.g. Abele, 1964, 1991, 1994; Ampferer, 1941;

Erismann *et al.*, 2013; Gruner, 2006; Leuchs, 1921; Matznetter, 1956; Penck, 1882; Poschinger *et al.*, 2006; von Poschinger, 2011). However, only a few researches focus explicitly on Toma Hills (Brunner, 1962; Imre *et al.*, 2010; Wolkersdorfer, 1991; Wolkersdorfer *et al.*, 2017). This study focuses on the Fernpass rockslide and the associated Toma Hills, which can be found in the Northern Calcareous Alps between the Lechtal Mountains in the West and the Mieminger Mountains in the east (Figure 1.1). The study of Toma Hills is described using an analogue (physical) laboratory scale model to understand their formation mechanism.

Toma Hills are morphological structures formed relating to some rockslides and one cannot recognize any system in their arrangement within the hummocky morphology of the rockslide deposit. Their name “Toma” originates from local language in Austria and Switzerland (Penck *et al.*, 1901), which in turn derives from latin *tumus* or *tumulus* (Staub, 1910). Abele (1974) defined them morphologically as “isolated cone-, pyramid- or roof-shaped eminences consisting mainly of landslide material with more or less smooth slopes of constant gradient” and explicitly excluded a genetic explanation. Staub (1910) adds that the Toma landscape is partly a result of fluvial processes and he describes cases where he sees Toma Hills clearly resulting from fluvial erosion. Yet, Nussbaum (1934) points out that “Toma” also occur “where a cutting and meandering river is missing”. In many cases, the Toma Hills consist of an outer covering with loose material and a core with harder or less fractured material, which was already noticed by the earliest authors (Sererhard, 1872). One exception, described in the literature, is the Bindschedler-Bühl near Chur, which consisted only of loose, unconsolidated material (Brunner, 1962). Internally the material can consist of both loosened and fractured rockslide material and moraines as well as crystalline erratica. Toma Hills are usually imbedded in a hummocky morphology, but not all the

hummocks in such a morphology can be classified as Toma Hills. The distinction between hummocks and Toma hills in this thesis differs from other authors.

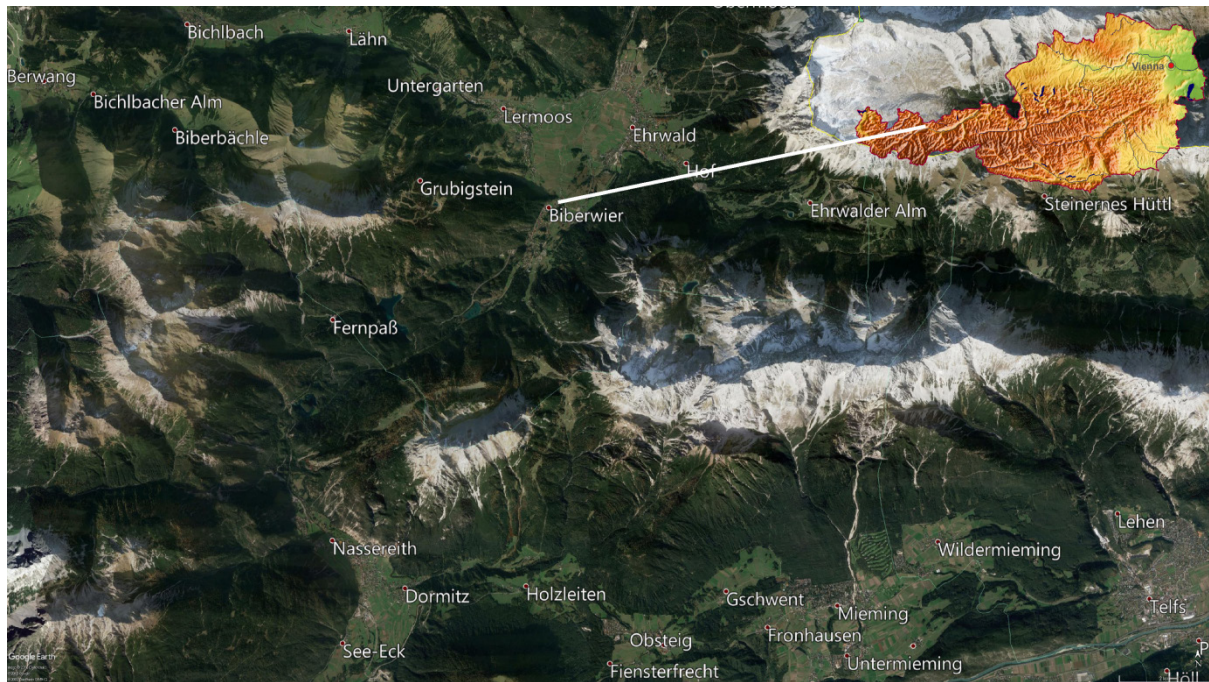


Figure 1.1: Overview of the study area. The Fernpass rockslide is slightly left of the centre of the map (© Google Earth, Wikipedia)

1.3 Problem statement and definitions

The formation of Toma hills has proved to be an ongoing discussion with multiple hypotheses behind it. Four hypotheses have been proposed so far: one of the first hypotheses was that Toma Hills are formed as a result of dead ice melting, and another one saw the Toma Hills formed in conjunction with the transportation of rockslide material on a still existing glacier. They were then followed by another hypothesis which is based on Karstification process. The area surrounding the Fernpass is characterised mainly by chemically sedimentary rocks, from dolostones to bituminous dolostones and gypsum and therefore this hypothesis is based on these types of rocks. The recent hypothesis is that the Hills were formed by transportation of rockslide material on liquefied, water saturated sediments. The concept that was used is that of inertial entrainment friction to support this hypothesis.

A more general review and discussion of the internal instability processes that occur in loose rock material has been given by Fannin *et al.* (2014), who present a summary of studies conducted to understand erosion of earth dams. In these engineering studies, internal erosion processes are a substantial threat to dam stability (Vazquez Borragan, 2014). Different groundwater velocities were exploited in the analogue experiments and identified if it is possible for groundwater to erode, transport and deposit different grain sizes resulting in an overprint of the rock debris, ultimately resulting in the formation of Toma Hills. As a matter of course, the analogue model – like any model – is an oversimplification of the reality (Box, 1979), but was designed to mirror the initial stage of the rock slide after the main sturzstrom came to a provisional rest. For example, the analogue model discussed here is not taking into consideration precipitation, snow or surface runoff. Though the Fernpass rockslide with all the lakes, hummocks and Toma Hills can be considered a small drainage basin, the principles first described in detail by Tóth (1963) about the various groundwater flows in small drainage basins will not be considered in the analogue model as well.

The internal structure of the Fernpass rockslide is dominated by a varying block-size separation and fragmentation with grain shapes ranging from subangular to well-rounded (Figure 1.2). This further implies that material making up Toma hills is of unconsolidated and unsorted debris with strongly varying grain sizes (Prager *et al.*, 2009a; Prager *et al.*, 2009b). It raises questions such as how fast groundwater is and was flowing through the rockslide debris and what groundwater velocity is required to erode, transport and deposit certain fragment sizes of the debris. Therefore, the time it takes for groundwater to move through the material, the groundwater velocity and

hydraulic conductivity of the material were crucial factors during the analogue laboratory study.

As indicated before, this study distinguishes between hummocks and Toma Hills. A hummocky rockslide morphology, like the one in figure 9.15 of Deline *et al.* (2015) or on top of the Heinleswald of the Fernpass rockslide does not imply that these hummocks have the same genesis as the Toma Hills. To ensure that there is no confusion between hummocks, which can have variable genesis, and Toma Hills, this study will deviate from the ambiguous usage in other similar studies (Dufresne, 2014; Dufresne *et al.*, 2015b; Paguican *et al.*, 2014). While this applies for the terminology, it does not apply for the explanations provided in the before mentioned studies.



Figure 1.2: The Fernpass rockslide internal structure (photographer: K.S. More)

Relating to internal erosion processes caused by flow or seepage of groundwater, the international terminology can be considered inconsistent. For the same phenomenon, authors are using “suffusion”, “suffosion” or other terms more or less interchangeably, which might be confusing for readers. Fannin *et al.* (2014) go one step further and point out that this “lack of clarity arising from use of the same term to describe these two distinct phenomena is an impediment to scientific progress”. They define that

suffusion entails mass loss, decreased hydraulic conductivity and no volume loss, whilst *suffosion* entails mass and volume loss and a change in hydraulic conductivity. The Toma Hill formation is discussed here in the context of mass and volume loss, and therefore the term *suffosion* describes the phenomena more precisely than *suffusion*.

1.4 The Fernpass rockslide and Toma hills

The Fernpass rockslide is one of the largest rock slope failures in the Alps and the area is characterized by a hummocky surface with Toma hills, which were formed after the rockslide event. The rockslide and related Toma Hills are located in the Northern Calcareous Alps, between Nassereith and Biberwier, about 42 km west-northwest of Tyrol's capital Innsbruck (Figure 1.1). Toma hills are characteristic landforms of many alpine rockslides characterized by a cone-like shape with a flattened tip, which are made of local mountain material (Abele, 1964; Staub, 1910). They have their scientific name from the local names of such hills from Switzerland (Penck *et al.*, 1901); the local names are also found in the Zwischentoren ("Dummabichl" north of Biberwier). Without mentioning details, their origin has been traced back to the following causes (Abele, 1964; Calhoun, 2015; Meili *et al.*, 2013; Mostler, 2013; Penck, 1882; Penck *et al.*, 1901; Poschinger *et al.*, 2009; Staub, 1910):

- Transport of rockslide material on an existing glacier
- Melting of glacier on rockslide material
- Fluvial
- Karstification
- Transport of rockslide material on liquefied, water-saturated sediments

However, none of these five hypotheses can account for *all* phenomena found on the site, and the first two have been sufficiently refuted in the meantime (Imre *et al.*, 2010; Meili *et al.*, 2013; Prager *et al.*, 2006a). Even against the purely fluvial origin, various authors have already given arguments early on and noted that not all connections between the mechanics and the formation of Toma hill are fixed. In particular, the “smooth, symmetrically arranged flanks and rectilinear sharp ridges” (Abele, 1969) cannot be explained conclusively with the previous models.



Figure 1.3: Overview of the Fernpass rockslide near Biberwier (in the left of the image). 1: rockslide source area, 2: Fernpass lakes, 3: northern branch of the rockslide with 4: selected Toma Hills. Direction of view to the south-west (photographer: Ch. Wolkersdorfer)

The Fernpass rockslide has been dated by three independent radiometric methods, ^{14}C -, ^{36}Cl - and $^{230}\text{Th}/^{234}\text{U}$ -dating, on which samples were collected at different places on the southern branch of the rockslide. The ^{14}C dating method yielded a minimum age of 4100 ± 1300 a and a $^{230}\text{Th}/^{234}\text{U}$ dating method produced an age of about 4150 ± 100 a (Prager *et al.*, 2009a; Prager *et al.*, 2008), which is older than the 2255 ± 60 a ^{14}C -age reported by Abele (1991) for a pine tree deposited in lacustrine material of the Kälbtertal. Rockslide material makes up Toma Hills but it does not mean they are

in their current form the same age as the rockslide. Actually, they might be younger because it takes time for the Hills to form after the initial rockslide.

The rockslide originated from a maximum elevation of 2231 müA, showing debris of a volume of about 1 km³. The material is about 100 m thick and split into two channelled sturzstroms with a length of up to 16 km. One of these Sturzstrom branches contains a larger debris volume when compared to the other one. The reason for the two channelled Sturzstrom branches is likely to have been caused by gravity and the force of the rockslide on partly liquefied fluvial sediments (Prager *et al.*, 2006a; Prager *et al.*, 2006b).

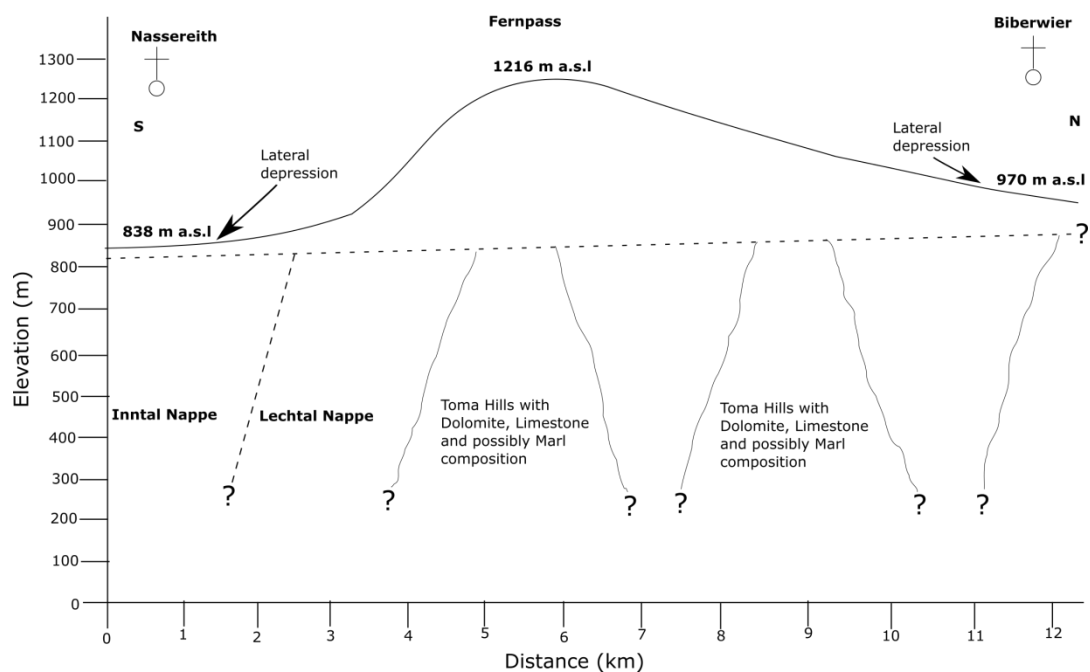


Figure 1.4: Schematic cross section in the Fernpass rockslide area

1.5 Hypothesis

Hypothesis, which is a combination of two previously proposed hypotheses about the formation of Toma Hills, is that Toma hills are a result of a combination of internal erosion, suffusion, Karstification and transportation of rockslide material on liquefied, water-saturated sediments (Figure 1.5). During hydrogeological mapping and field

investigations around Biberwier, in the northern branch of the Fernpass rockslide, some characteristics were noticed, some of which had already been described by previous researchers: (1) in some valleys between Toma Hills, flowing groundwater can be heard occasionally and (2) the angles of the Hill flanks correspond to the natural fill angles of the respective material of which the Hills are formed (pers. comm. Wolkersdorfer, 2016). Consequently, the formation of Toma Hills will be discussed here in the context of mass loss due to erosion and the accompanied internal instability of the rock debris (“sediment”).

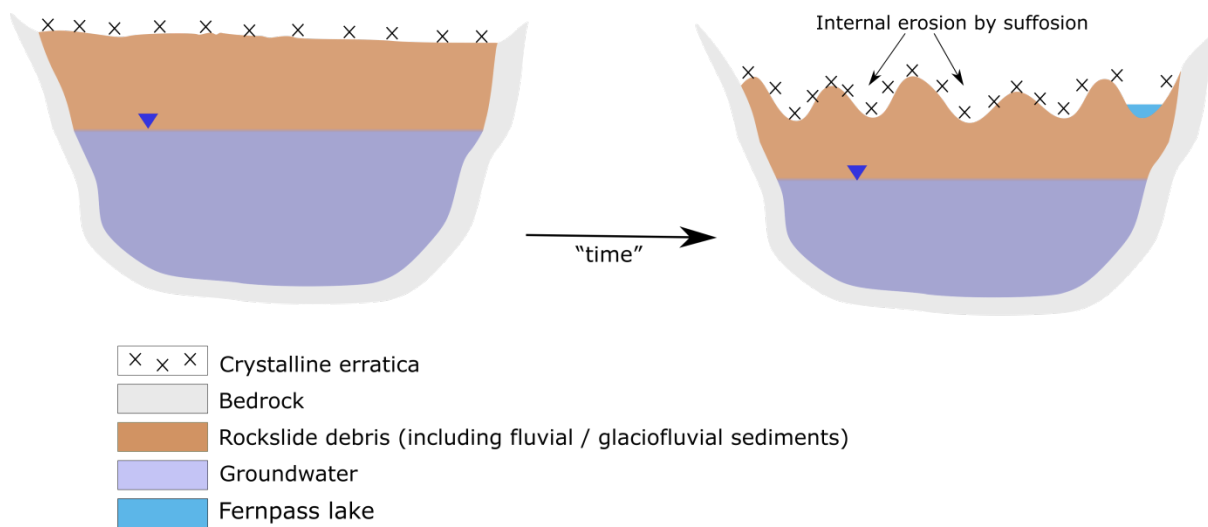


Figure 1.5: Conceptual model of the processes involved in Toma hill formation. Not to scale.

1.6 How can all of the Toma hills features be explained with the current knowledge

So far, four hypotheses have been proposed for the formation of Toma hills. However, these hypotheses cannot explain all the Toma hills features. According to Abele (1964), material making up Toma hills include Tillite and this would mean that Toma hills formed during glaciation age. Three independent radiometric dating methods were used to date the rockslide and yielded a minimum age of at least 4000 a, but the end of the last glaciation was 10 000 a ago (Giner *et al.*, 2015; Prager *et al.*, 2008).

Therefore, this implies that Abele's hypothesis cannot explain all the Toma hills features.

Toma hills are well shaped and this raised questions such as whether the shape comes from melting of glacier on the rockslide material that formed the hills or not (Abele, 1964). According to the current knowledge, the shaping might come from internal erosion due to groundwater flowing in some parts of the Fernpass rockslide area.

1.7 Objectives of the study

The main objective of the present study is to investigate the potential contribution of internal erosion by suffosion due to the presence of groundwater flow in the formation of Toma hills. Based on this objective, the following activities were carried out to achieve the main objective:

- Constructed a laboratory scale analogue model to investigate the potential Toma hills formation by internal erosion by suffosion,
- Investigated the processes having formed Toma hills on a laboratory scale by varying the grain sizes and groundwater velocity,
- Investigated groundwater velocity required to move different material and the sizes of all possible rock fragments that formed Toma hills, and
- Used hydrogeological principles to relate groundwater velocity to different grain sizes.

CHAPTER 2

2 Site Description

2.1 Regional geology

Geologically, the area surrounding the Fernpass is mainly characterized by shallow-marine dolostones of the Norian Hauptdolomit (Upper Triassic) and the bituminous Upper Norian Seefeld Formation which makes up the younger successions of the monotonous Hauptdolomit (Prager *et al.*, 2009b; Schmid *et al.*, 2004). These rocks are distinctive of its grey-white colour in the Northern Calcareous Alps (Figure 1.3). In addition, the area contains metamorphosed crystalline rocks such as marble, quartzite and amphibolite on top and within the rockslide material, called crystalline erratica. Today, the Fernpass high is the water divide between the river Inn in the south and the Danube (Donau) in the north.

2.2 Structural geology

One characteristic of the Fernpass rockslide is the convex transverse profile of the debris, which is a result of a relatively small head difference between the Afrigall (source of the rockslide) and Biberwier (Abele, 1974). This convex profile gives way to small marginal valleys (“Randtälchen“) on both sides of the debris, in which small rivulets flow (e.g. Loisach, Dorfbach). In addition to the morphological feature of Toma Hills, the Fernpass rockslide is characterized by morphological depressions which are interpreted as karst dolines (Abele, 1964).

Mostler (2013) recently proposed that these dolines are indicative for gypsum karst and consequently the whole Fernpass area is not a rockslide but a result of karstification, a hypothesis already proposed by Penck (1882) and refuted since then.

Yet, as Abele (1974) pointed out, the debris of the Vajont Valley rockslide showed doline-like structures caused by either internal erosion or by sagging of the unconsolidated material. These doline-like structures can be seen at the Vajont Valley rockslide front slope in many early images. It could therefore be that the doline-like structures at the Fernpass also result from physical erosion rather than chemical erosion.

2.3 Climate and vegetation

With reference to the Austrian travel guide website, the weather in the area is highly influenced by the Atlantic climate due to it being in a temperate region. All the four seasons have unique cold and hot seasons, causing the area to have highly unpredictable weather patterns. The variety in weather is largely because of the geology of the area; therefore, this divides the area into three climatic regions known as the East, Alpine regions and other areas. The study area falls under the Alpine regions notorious of its high precipitation short and long summers and winters respectively.

Austria experiences enough rainfall and due to this it is highly characterised by forests. Therefore, the country has minimal chances of experiencing rockfalls or landslides due to gravity. The triggering mechanism for rockslide events in this area is therefore the stream flows. This is discussed more in details in the following chapters.

CHAPTER 3

3 Literature Study

3.1 Rockslide movement and factors influencing the occurrence of a rockslide

Factors that normally influence the occurrence of a rockslide typically include the slope angle, slope stability, water content of the rocks, erosion, weathering, overloading, gravity and the geological setting. Some of the above-mentioned variables also control the geometry of the failure surface and its advancement both in space and time. Since the earliest studies of alpine rockslides, various models and hypotheses have been displayed to clarify the areas of substantial slope failure, activating processes, rates and sorts of development, time of event, their geometry and their effects including, for instance, effects on structure and expanded disintegration (Abele, 1964; Imre *et al.*, 2010). Especially Imre *et al.* (2010) and Meili *et al.* (2013) conducted and published results of laboratory experiments of the Toma Hill formation resulting from physical processes causing fragmentation of the Sturzstrom (rock avalanche) debris.

Pouliquen *et al.* (1997) and recently Valderrama *et al.* (2018) conducted analogue models to study fingering that might occur at rock slides. In one of the experiments, indication for the formation of Toma-Hill-like structures was encountered. Instead, their experiments explained ridges, which are not evident at the Fernpass rock slide, though Dufresne *et al.* (2009) list them in their table 1, referring to Abele (1964). Shea *et al.* (2008) studied the difference between the development of ridged or hummocky morphology by means of numerous laboratory experiments. They found that “the analogue model demonstrated that collapses composed of initially heterogeneous

materials [...] tend to generate hummocky surfaces”, while “dominantly fine grained and homogeneous granular material slides” caused dominantly ridged structures (Shea *et al.*, 2008). None of their results specifically explains the formation of Toma-Hill-like structures.

Numerical models were conducted by Gramiger *et al.* (2016) in order to study the run-out of two rock slides in the Swiss Bernese Alps. Though hummocky surfaces appear in the nature and in the model, none of them can be considered Toma Hills and their model, consequently, can't be used to understand the Toma Hill formation in more detail.

There are several cases of dry rock slides or rock falls, where the separation of the fragments occurs even when the vertical drop of the material is comparably narrow. These rockslides might become sturzstroms as the movement controlling intergranular coefficient of friction might become less. Sturzstroms are rockslides of extended volume compelling run-out which show concentrated discontinuity of blocks of rock because of the collision of rocks during the rock debris movement (Heim, 1932; Hermanns, 2013; Imre *et al.*, 2010; Prager *et al.*, 2006b). Though a number of causes will contribute to a rockslide, there is one, which ultimately triggers the movement of material, in most cases: fluvial erosion as the dominant process because it is linear, regressive and connected with convergent valley streams (Abele, 1994). The Fernpass rockslide material and area are dominated by chemically sedimentary rocks, stream channels and groundwater flow within the debris. Therefore, it may be possible that carbonate rocks in the area may have been fractured along bedding planes, and because of the presence of stream, fluvial erosion may have played a role in triggering the Fernpass rockslide (Mostler, 2013; Penck, 1882).

Some rockslides have the ability to travel a long way from the source of the initial fall. The debris and rock fragments from rockslides can range from tiny grains to boulders, and some boulders tend to break up into smaller pieces as the slide moves down the slope and large pieces collide with each other (Prager *et al.*, 2005). A hummocky morphology, which on first sight seems to be similar to the Toma Hill landscape, also formed in conjunction with the debris avalanches of the Iriga volcano, Philippines (Capra, 2011), and Reiser *et al.* (2010) pointed out that sometimes even moraines might be confused with Toma Hills. Yet, the movement of the Fernpass rockslide and several other rockslides have proven to be unusual and maybe the explicit reason for confusion of the formation of Toma Hills.

During the movement of rockslide deposits, processes such as lithification and diagenesis take place (Figure 3.1). The Fernpass Sturzstrom contains solid rocks which may have formed when sediments compacted under pressure (lithification), and they changed during and after lithification (diagenesis) (Sanders *et al.*, 2010).

As the slope failure occurs and the debris slides into the valley, the movement of the rockslide debris will be supported by water-saturated sediments. This kind of movement can travel long distances and spread wide because of a mixture of sand, gravel, silt and water (Abele, 1997). However, the movement will stop after some time and this will cause material to pile up on each other and form hills (Figure 3.2). A larger volume of rock slope failure result in a long run-out distance than a smaller volume of rock slope failure. Most of the rockslides (Flims, Tschirgant, Sierre, Köfels and Obernberg rockslides) in the Alps region are associated with this type of movement, rockslide debris interacting with fluvial sediments, and the travel distance is long (Abele, 1997).

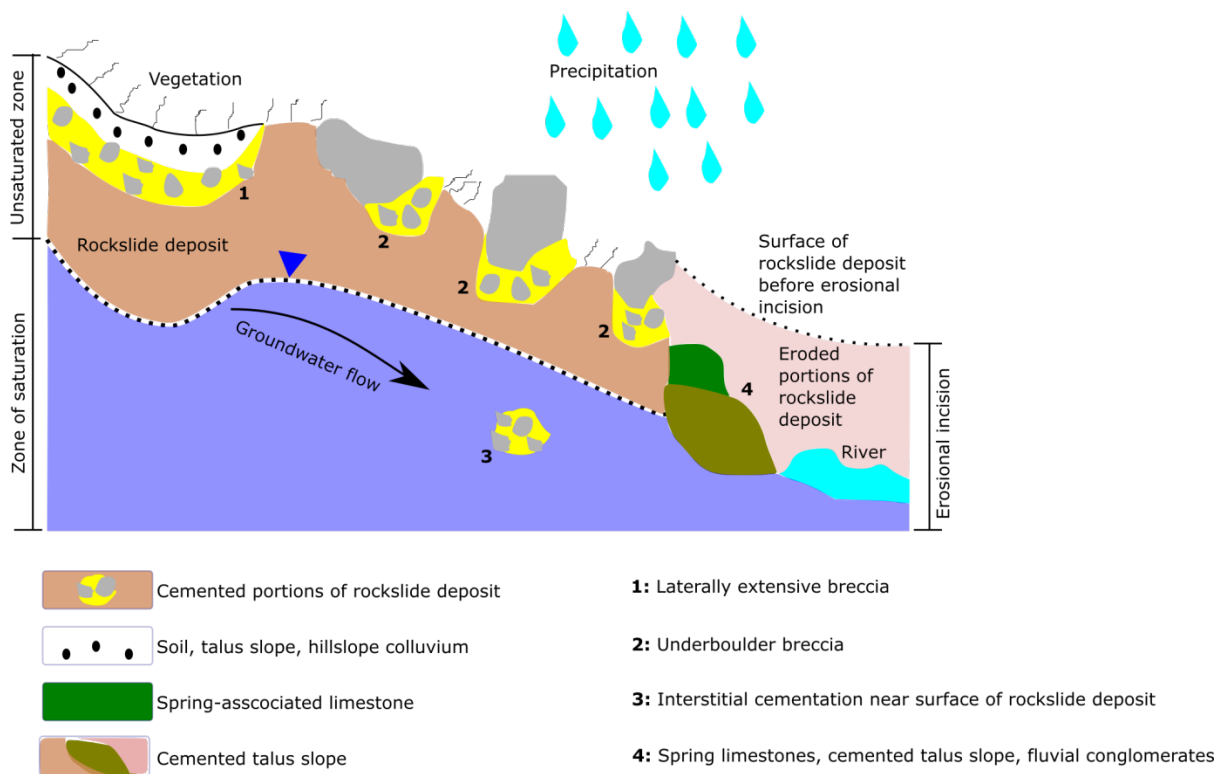


Figure 3.1: Diagenetic features associated with carbonate-lithic rockslide deposits. Not to scale (after Sanders *et al.*, 2010)

By determining the expected volume and the difference between the lowest point of the depositional area and the highest point of the head scarp we can be able to predict the run-out distance of the rockslide debris (Abele, 1997; Legros, 2002). However, not all the predictions are always correct. Processes involved in this type of movement are quite easy to follow; as the rock slope failure occurs, rockslide debris will then move over fluvial sediments, ranging from fine grained to gravel, exerting force upon the sediments. This kind of motion occurs fast and then blocks the escaping way for pore water and the pore water will support part of the weight of the rockslide by acting as a lubricant (Abele, 1997).

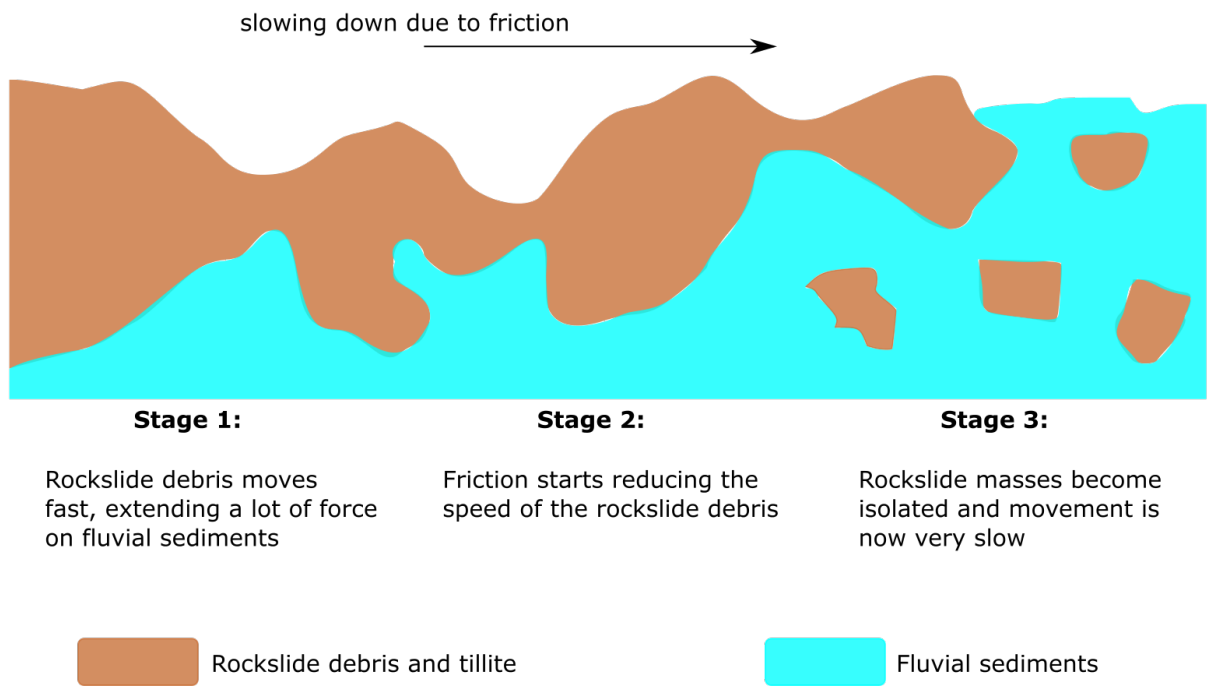


Figure 3.2: Rockslide debris movement illustrated in three stages. Not to scale.

Looking at the lowest parts of the valleys around most of the Alps rockslides, it is safe to say that they are largely covered by deposits from rockslides (Figure 3.3). These deposits range from well sorted to poorly sorted, from fine grained to boulders, and are several metres thick. According to the current knowledge, Toma hills are made up of the rockslide sediments (Prager *et al.*, 2009a).



Figure 3.3: Rockslide sediments in the Fernpass rockslide valley. The size of the book is 22×15 cm (photographer: K.S. More)

3.2 Other Alps rockslides associated with Toma hills

With respect to the reviewed literature, all of these rockslides are connected to Toma hills in a similar mechanism, i.e. material detaching and coming into contact with glaciofluvial sediments. During the occurrence of the Flims rockslide when $\approx 12 \text{ km}^3$ of material, mainly limestone, detached from the northern side wall of the Vorderrhein river valley, just about $\approx 1 \text{ km}^3$ sediments in the valley were impacted and liquefied. This led to an immediate mudflow, and travelled for a distance of approximately 16 km downslope, coming into contact with large material of the rockslide debris and eventually forming Toma hills. Material of Toma hills in the Swiss Alps ranges from cobble gravel to sand (Calhoun, 2015; Crosta *et al.*, 2009; Wassmer *et al.*, 2004).

The mass of the Tschirgant rockslide also got liquefied as it slid into the river Ötz and travelled a long distance to carry large rock fragments, leading to Toma hills formation. The hills are characterized by strongly varying grain size distribution, ranging from sand to cobbles (Abele, 1997; Dufresne *et al.*, 2015a; Dufresne *et al.*, 2015b). With

similar mechanism, lake Obenberg is associated with the material of the Obenberg rockslide, while river Ötz also liquefied the Köfels rockslide material, and the material of the Sierre rockslide slid in the Rhône river (Ivy-Ochs *et al.*, 1998; Körfgen *et al.*, 2014; Ostermann *et al.*, 2012; Ostermann *et al.*, 2013; Pánek *et al.*, 2016; Pedrazzini *et al.*, 2013).

3.2.1 Flims rockslide (Switzerland)

The Flims rockslide is the largest rockslide in the Alps, with an estimated volume of about 9 – 12 km³. It is situated in the south eastern Swiss Alps in the canton of Graubünden, Switzerland, on the north slope of the Vorderrhein valley, Upper Rhine river valley (Wassmer *et al.*, 2004). The rockslide happened from a high speed movement of a large limestone mass, and several factors contributed to the occurrence of this rockslide (Crosta *et al.*, 2009):

- The steep rocky slopes of the Rhine river valley
- Frictional forces resulting from the rockslide debris and the ground which it was moving on
- Shaping of rock fragments as the rockslide debris continue to move

Radiocarbon dating method was used to date the Flims rockslide, and the boulders of the rockslide debris and the bedrock yielded a minimum age of 15340±1490 a to 15440±1480 a. This age was supported by the age of the deglaciation of the Segnes valley that were obtained on the surface of the bedrock just outside of the rockslide area – it was dated to be about 11410±590 a and 13340±1090 a (Ivy-Ochs *et al.*, 1998). Therefore, the Flims rockslide occurred during temperature changes (melting of glacial ice) in the early Holocene (Crosta *et al.*, 2009).

The rockslide debris slid in the Upper Rhine river valley on liquefied, water-saturated sediments, and the movement evolved quickly into a Sturzstrom that was 10 km long

and 400 m in height. This Sturzstrom is one of the largest movements in the Alps and possibly on Earth because of the high volume of rocks involved (Wassmer *et al.*, 2004). The Sturzstrom travelled about 11 km with the deposits blocking the Vorderhein valley, forming a large lake and small Toma hills, consisting of Helvetic rock material (Poschinger *et al.*, 2009; Wassmer *et al.*, 2004).

The internal structure of the Flims deposits can be divided into five types of facies: structured facies, intermediate facies, granular facies, brecciated facies and washed facies, with respect to their location within the Sturzstrom mass (Pollet *et al.*, 2000; Wassmer *et al.*, 2004):

- Within the internal parts and the proximal of the rockslide deposits lies well-structured facies. It is made up of a variety of grain sizes, from gravel to boulders. According to Schneider *et al.* (1999), the preservation of the internal structure seems to correspond to the early movement of the Sturzstrom.
- Intermediate facies is composed of rock fragments in a granular matrix and it form the top part of the rockslide deposits.
- A granular facies consist of rock fragments in a sandy matrix and it can be found at the surface of the deposits.
- Rockslide debris slid on the foot of the slope of the Rhine valley and this is where a brecciated facies can be found. It's made up of highly angular clasts in a sandy matrix.
- At the surface of the deposit a washed facies can be seen. The grains are rounded to well-rounded and this is due to the water flow in the Rhine river valley.

3.2.2 Tschirgant rockslide (Austria)

The Tschirgant rockslide area is situated at the southern margin of the Northern Calcareous Alps in Tyrol, Austria. The rockslide produced debris of a volume of about 0.2-0.25 km³. The Tschirgant ridge is about 2370 müA, and the area surrounding the Tschirgant is characterised by massive to thick-bedded, intensively fractured limestones and dolostones of the Wetterstein Formation in contact with well-bedded carbonates of the Alps Muschelkalk Group (Dufresne *et al.*, 2015a; Dufresne *et al.*, 2015b, Figure 3.4).

Three independent radiocarbon dating methods were applied to different samples from different locations (buried wood in the rockslide deposits near Sautens and buried soil remnants at the base of the rockslide deposits near Ambach) and produced an age of about 2900 a BP (Abele, 1997; Dufresne *et al.*, 2015a). However, though different ages for the Tschirgant rockslide were found through multiple investigations all date the rockslide into the middle Holocene (Table 3.1).

Table 3.1: Ages for the Tschirgant rockslide from different investigations and methods

Radiometric Method	Sample	Age
¹⁴ C-dating	Different wood/charcoal fragments	2900 ¹⁴ C BP (c. 1050 BC)
²³⁴ U/ ²³⁰ Th-dating	Post depositional carbonate cements	3650±350 a and 2800±100 a
¹⁴ C-dating	Different wood/charcoal fragments	3650-3450 cal. a BP and 3070-2950 cal. a BP
³⁶ Cl-dating	Boulder surface exposure	2980±500 a

There are several factors influencing the occurrence of a rockslide, and it was proved through investigations that the Tschirgant rockslide was caused by a failure of a highly

deformed carbonate rock mass on the south eastern face of a ridge that is 2370 müA. The rockslide debris slid on the fluvial sediments in River Ötz and moved southward in this liquefied, water-saturated valley fill while a much smaller volume of this debris moved northward in a water-saturated fill of the River Inn (Abele, 1997; Dufresne *et al.*, 2015a; Dufresne *et al.*, 2015b). Material making up the debris varies from clay to boulders, rounded to sub-angular fragments (Prager *et al.*, 2008).

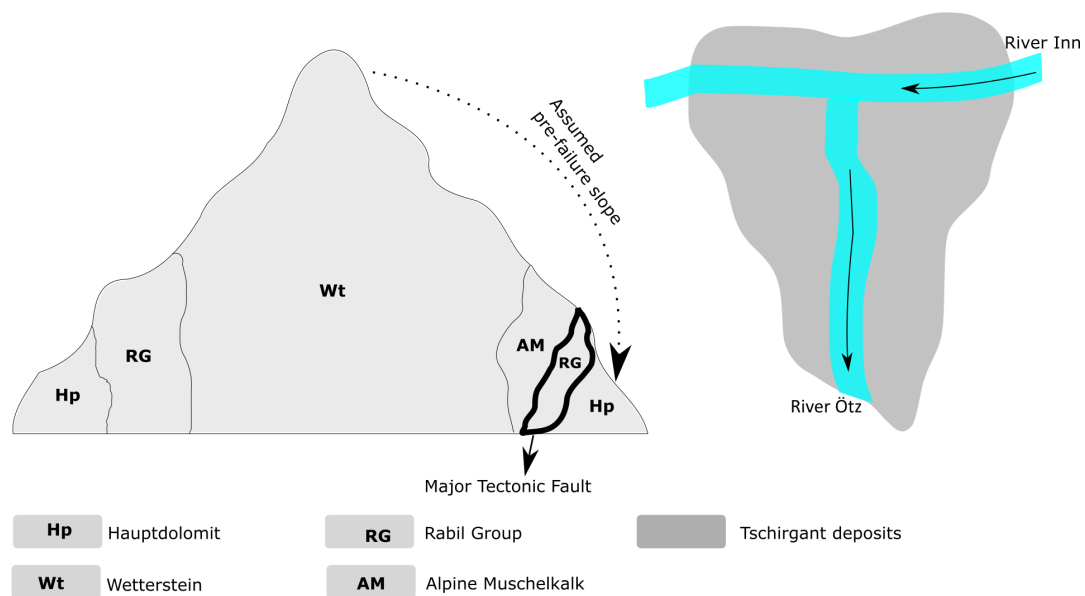


Figure 3.4: Conceptual drawing and cross section of the Tschirgant ridge on the left side and the shape of the Tschirgant rockslide on the right side. Not to scale.

3.2.3 Köfels rockslide (Austria)

The Köfels rockslide is located in the Ötztal valley in Tyrol, Austria, and represents one of the largest rockslides in the crystalline Alps. Its area is characterised by metamorphic rocks, mainly granitic gneiss (Körffgen *et al.*, 2014). The slope failure produced a volume of about 2 km³ of granitic gneiss that slid across and blocked the valley of the Ötz River (Ivy-Ochs *et al.*, 1998; Körffgen *et al.*, 2014). Several methods were used to date the rockslide (Table 3.2) and the ages proved that the rockslide occurred in the early Holocene after the last main glaciation (Ivy-Ochs *et al.*, 1998).

Table 3.2: Ages for the Kofels rockslide from different methods.

Method	Sample	Location	Age
Radiocarbon dating	Two pieces of wood	Tauferberg	8710 ± 150 ¹⁴ C a BP and 8750 ± 25 ¹⁴ C a BP
Accelerator mass spectrometry methods	Pieces of wood	Tauferberg	8705 ± 55 ¹⁴ C a BP
1993 dendro-calibration data set	Pieces of wood	Tauferberg	9800 ± 100
Analysing ¹⁰ Be and ²⁶ Al content in rock samples using AMS	Four quartz veins from boulders	The toe of the rockslide near Wolfsegg (Taufenberg)	8880 ± 490, 9680 ± 750, 10070 ± 520, 10630 ± 570
¹⁰ Be content using AMS	Boulder	The foot of the rockslide scarp	7430 ± 500
¹⁰ Be content using AMS	Brecciated quartz vein	The foot of the rockslide scarp	5880 ± 450

The rockslide debris consists of coarse material, from gravels to cobbles, in a matrix of soil containing a small amount of organic material. It slid into the Ötz River moving from west to east. Its debris is characterised by Frictionite and the hypothesis is that the friction between moving granitic gneiss debris and fluvial sediments created enough heat to fuse rocks to form Frictionite (Hyalomylonite), which is the favoured hypothesis. Two more, meanwhile outdated hypotheses are that the reason for Frictionite is because of volcanic activity or a meteorite (Ivy-Ochs *et al.*, 1998).

3.2.4 Sierre rockslide (Switzerland)

The Sierre rockslide is a large rockslide in the Alps, involving a volume more than 1.5×10^{-9} km³. It is situated in the Swiss Alps in the middle part of the canton Valais in the South-western part of Switzerland. The rockslide deposits slid into the Rhône River, one of the major rivers in Europe, passing through Switzerland and France, and travelled a distance of about 12 – 14 km (Figure 3.5, Pánek *et al.*, 2016; Pedrazzini *et al.*, 2013).

The area surrounding Sierre is characterised by soft greyish limestone that crumbles easily, marl and calcareous schist of the Valanginian age, micritic limestone of the Valanginien Supergroup and Hauterivien Siliceous limestone. With reference to the exposed outcrop in the area, the dominating geological structure is faulting – the outcrops show relatively low dip angle characterising the faulting in the area as thrust fault (Pedrazzini *et al.*, 2013). Faulting might have also played a substantial role in the occurrence of the Sierre rockslide.

The radiocarbon dating method, ¹⁴C-dating, performed using mass spectrometry, was used to date the rockslide and yielded early Holocene age (Pedrazzini *et al.*, 2013, Table 3.3).

Table 3.3: Age of the Sierre rockslide from ¹⁴C-dating

Method	Sample	Location	Age
¹⁴ C-dating performed using atomic mass spectrometry	Two pieces of wood recovered during construction of the Hubil road tunnel	5 m and 30 m below the surface of the Hubil road tunnel	Deeper sample yielded 8620 ± 40 BP and shallower sample yielded 8550 ± 40 BP

Like many other rockslides associated with Toma hills, Sierre rockslide debris slid on soft, liquefied water-saturated material of the Rhône River (Pedrazzini *et al.*, 2013). This soft material plays an important role in the formation of Toma hills (Imre *et al.*, 2010). The traveling distance that is covered by the Sierre rockslide debris on the bottom of the valley is likely to be because of the mobilisation of the valley fill, which is also true for the Fernpass rockslide debris (Abele, 1994).



Figure 3.5: Overview of the Sierre rockslide (© Google Earth)

3.2.5 Obernberg rockslide (Austria)

The Obernberg rockslide is situated in the Austrian Alps, south of Innsbruck in the Obernberg valley. Obernberg valley extends towards Italy in the Schwarze Wand Mountain and the Tribulaun mountains (Figure 3.6). Initial rock volume of the slope failure was about 7.2 km over a 1330 m vertical distance (Fahrböschung of the rockslide is estimated to be 0°), and the rockslide deposits cover an area of approximately 3 km² (Ostermann *et al.*, 2012; Ostermann *et al.*, 2013).



Figure 3.6: Obernberg rockslide location (© Google Earth)

Obernberg rockslide is also a large Alpine rockslide, and it resulted from a range of processes and controlling features which makes dating complicated (Hutchinson, 1988). Radiocarbon dating was applied on organic remains in an alluvial fan down lapping the rockslide and yielded a minimum age of 7785 ± 190 cal. a BP. Another dating method, ^{36}Cl -dating, was used on boulders of the rockslide mass and provided a minimum age of 8.6 ± 0.6 ka BP which implies that the rockslide occurred during the early Holocene (Ostermann *et al.*, 2013). During palaeoclimatic investigations it was noticed that there are no records of glacial ice on the rockslide debris. Therefore, a lake found on the rockslide area was not formed by dead ice melting as assumed by previous researches (Ostermann *et al.*, 2012; Ostermann *et al.*, 2013). Rockslide debris shows evidence of long-distance run-out. The deposits from the slope failure slid in Lake Obernberg and moved up slope possibly forming Toma hills (Figure 3.7).

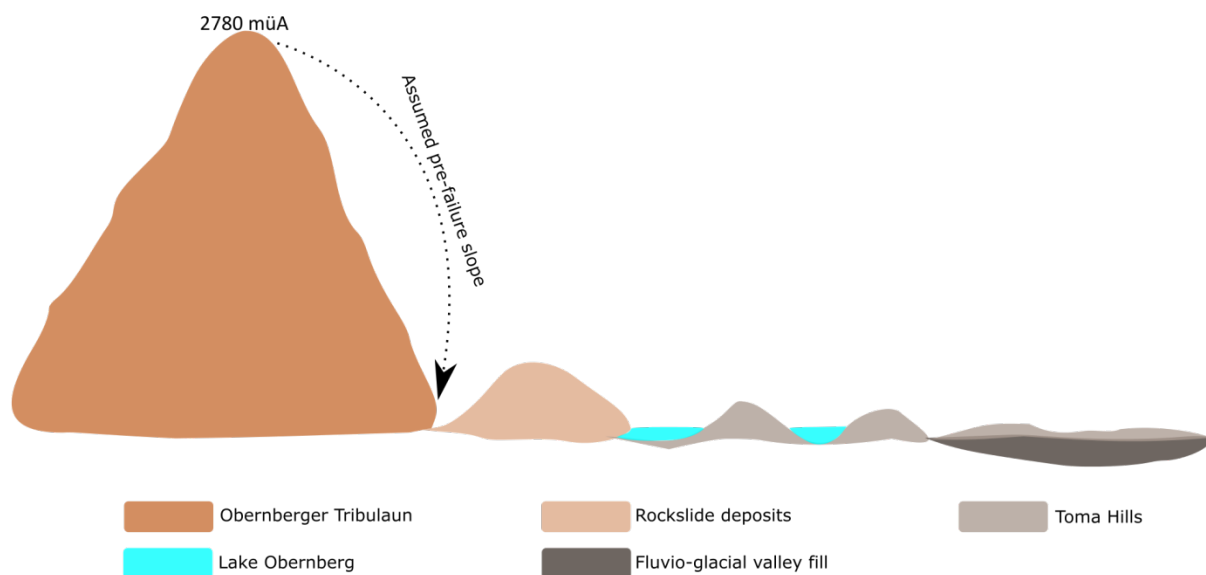
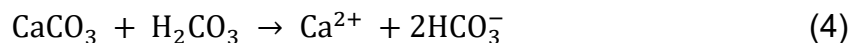


Figure 3.7: Movement of the Obernberg deposits. Not to scale.

3.3 Previously proposed hypotheses for the formation of Toma hills

3.3.1 Karstification resulting in the formation of Toma hills

The first paper to propose that Toma hills result from karstification is from Penck (1882), and the latest one about this hypothesis from Mostler (2013). Chemical weathering and attrition of carbonate rocks (limestone, dolostone, marble) result in karst landscapes. The main influencer is acidic ground or soil water, which will form carbonic acid, and this acid will dissolve the carbonate rocks (Aranburu *et al.*, 2015). Karst landscapes are characterised by lack of freshwater activity, absence of vegetation and sometimes the presence of sinkholes. They are an important and an obvious feature for identifying karst landforms. When acidic water dissolves carbonate rocks, it leaves voids of small to big sizes in the ground, and the roof will eventually collapse forming sinkholes (Aranburu *et al.*, 2015; Mostler, 2013). The reaction steps involved in carbonate rock dissolution are as follows:



The area surrounding the Fernpass is characterised mainly by chemically sedimentary rocks, from dolostones to bituminous dolostones and gypsum, and therefore this hypothesis is based on these rock types (Prager *et al.*, 2009a). According to Penck (1882) and the newer opinion by Mostler (2013), karstification caused the shape of the Fernpass area and Toma hills.

3.3.2 Transportation of rockslide material on a still existing glacier

According to Abele (1964), Toma hills result from the transportation of rockslide material which piled up on a still existing glacier. He further proposed that the movement of the rockslide material was controlled by a moving glacier. Moving glaciers result in erosion of the underlying rocks and the resulting debris is of silt to boulders (Sam *et al.*, 2015). The underlying rocks and material are picked up by the moving glacier and are locked in the ice (Figure 3.8).

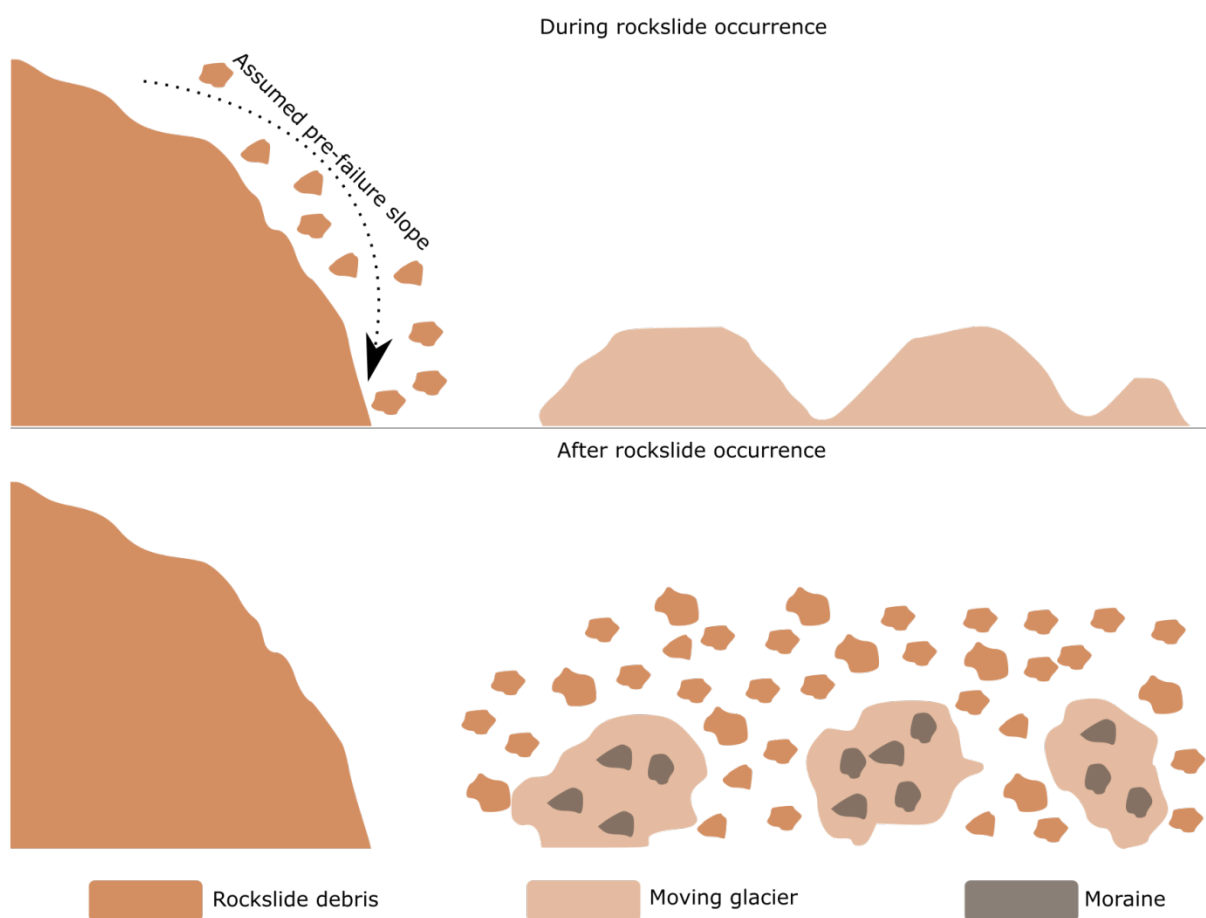


Figure 3.8: Schematic illustration of Sturzstrom supported by moving glacier. Not to scale.

Material that's stuck in the ice is called "moraine", and this material enables the glacier to erode the underlying material. Traveling of rockslide material over a glacier produces a higher speed and reaches long-run-out distances. Not only would a glacier

influence the run-out of the rockslide debris, it also changes its structure (Deline *et al.*, 2015). Rockslide deposits that are characterised by glaciers are difficult to date and to track their movement (Deline *et al.*, 2015; Sam *et al.*, 2015).

3.3.3 Formation of Toma hills due to dead ice melting

Another hypothesis proposed by Abele (1964) suggests that the shape of Toma hills is due to dead ice melting on the rockslide material. This simply means that the glacier held the rockslide material together, transported and deposited it. The depositional mechanism for this material is that the glacier melts after a long-run-out distance and releases the rockslide material, making it pile up on each other to form Toma hills. This hypothesis is much more like the previous one, "Transportation of rockslide material on a still existing glacier", in terms of movement. The melting glacier in this case will then act as a lubricant for the movement of material (Abele, 1964). However, these two hypotheses can be considered outdated at present because the structure of Toma hills resembles that of a rockslide and is not shaped by the late glacial ice as assumed formerly.

3.3.4 Transportation of rockslide material on fluvial sediments

The recent hypothesis about the formation of Toma hills is that of Imre *et al.* (2010) and Abele (1997) when they proposed that Toma-hills were formed by transportation of rockslide material on liquefied, water-saturated sediments (Figure 3.9). They used the concept of inertial entrainment friction to support their hypothesis. The Sturzstrom was made up of different Fernpass rockslide material, from silt to boulders, while the soft ground on which it moved on consists of liquefied water-saturated sediments of a hypothetical river Loisach. This kind of movement triggered a very high friction which slowed down the Sturzstrom movement and formed the hills as the rockslide material piled up (Imre *et al.*, 2010).

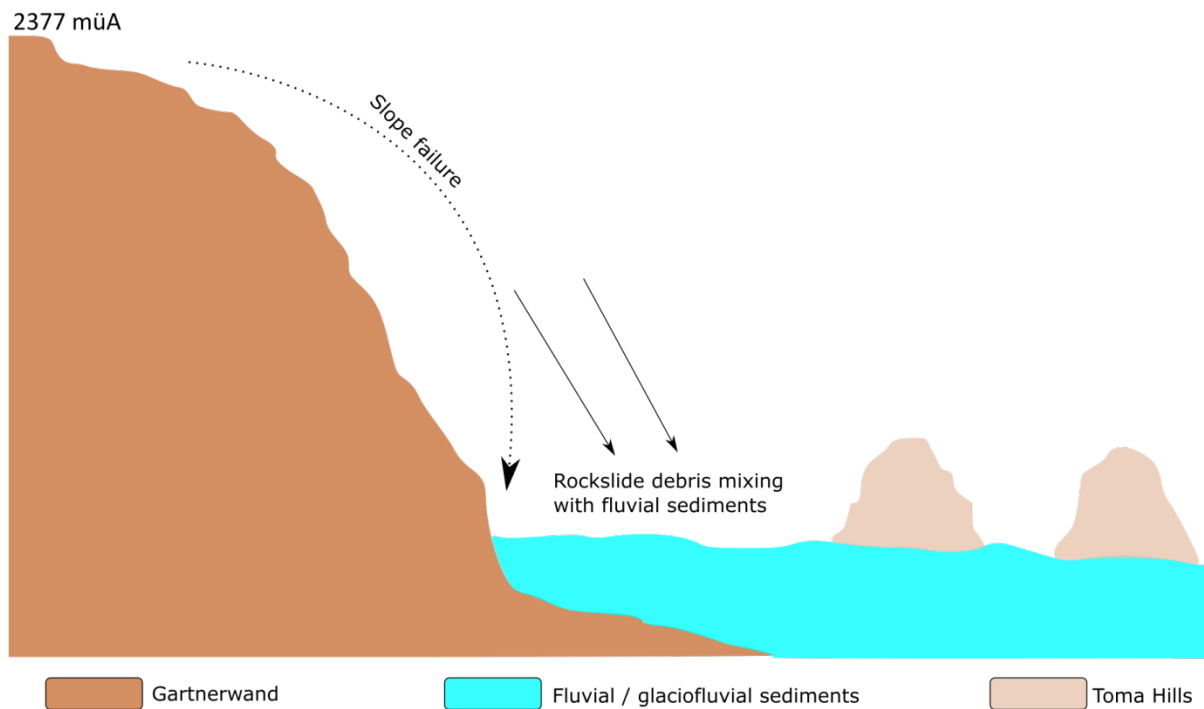


Figure 3.9: Schematic illustration of how rockslide debris mix with and trail on fluvial sediments to form Toma hills. Not to scale.

The mountains, Gartnerwand and Kreuzjoch, on which the slope failure occurred, were and are still relatively dry and this would make the rock mass dry. The Fernpass rockslide material shows long-runout distance, and this is difficult to understand due to the dry rock mass (Imre *et al.*, 2010). Therefore, for the rock mass to have such a long-runout distance it must have been supported by fluvial sediments with water acting as a lubricant.

CHAPTER 4

4 Methods and Materials

4.1 Experimental design: Analogue model

Analogue or physical modelling is commonly used in geological studies when it comes to understanding geological processes and time scales, especially in the context of CCS (carbon capture and storage) and radioactive waste disposal (Higgs *et al.*, 2015; Smellie *et al.*, 1997). As the Toma Hill formation took a long time to complete, possibly hundreds to thousands of years, the model was chosen such that this process could be studied in the laboratory. Consequently, an analogue groundwater flow model (“physical model”) was designed to understand the contribution of internal erosion by suffosion in the formation of Toma Hills. This approach was chosen as it allows to modify the water movement in such a way that it can be seen how the groundwater within the model travels.

The analogue model comprises of a rectangle 150 × 100 × 80 cm polyethylene tank (Pioneer Plastics, Rosslyn, South Africa) with nine inlet points at three different elevations to allow for the adjustment of the hydraulic gradient (labelled I₁ to I₉ at the front of the tank) and three outlet points (labelled O₁ to O₃ at the back of the tank) to force the direction and flow rate. Inlets were used for water inflow and outlets for water and eroded material discharge (Figure 4.1). This setup allowed for varying the flow conditions within a large range of conditions.

A 60 L container was placed adjacent to the outlets and used as a reservoir and to collect the eroded, finer material. Peristaltic pumps (Heidolph PD 5006, Schwabach, Germany) were used to circulate water from the reservoir to the chosen inlet point(s),

and the calibrated pump speed was adjusted until the inflow equalled the outflow volume. The tank was raised 4 cm at the inflow side to provide an initial hydraulic gradient. In all five experiments, an average of 0.98 m³ of loose (1.52 t, bulk density of 1.56 g/cm³) or 0.75 m³ of compacted (1.52 t, bulk density of 2.03 g/cm³) evenly mixed sand and gravel was used. After completely filling the tank with the material, Ca-Mg-HCO₃-type, Pretoria tap water was passed through the synthetic rockslide material under ambient temperature (15 – 25 °C) by means of two peristaltic pumps.

Each experiment had a duration of ± 30 days and the flow rate was adjusted between 0.9 and 1.7 L/min with an average hydraulic gradient of 0.24, not too different from the natural hydraulic gradient of 0.2 between the Hiendleswald (± 1300 müA) and Biberwier (± 990 müA).

4.2 Material selection and properties

Using the 45 sieve analyses of the sediments from the northern Fernpass branch, which Schuch (1981) analysed in three boreholes (Figure 4.2), a method for comprising a synthetic rockslide sediment for the experiment was developed. From the sieve analysis results, the average and median of all sieve analyses was calculated and to exclude outliers, the median values were used for composing the synthetic rockslide material (Table 4.1). This proved to be a great simplification of the actual sedimentological composition of a Toma Hill (Table 4.2), especially because the sieving method used by Schuch (1981) tends to result in smaller size fractions compared to the real situation (pers. comm. H. Mostler, 2017). In addition, as we were only interested in the physical erosion, inert sediment was used.

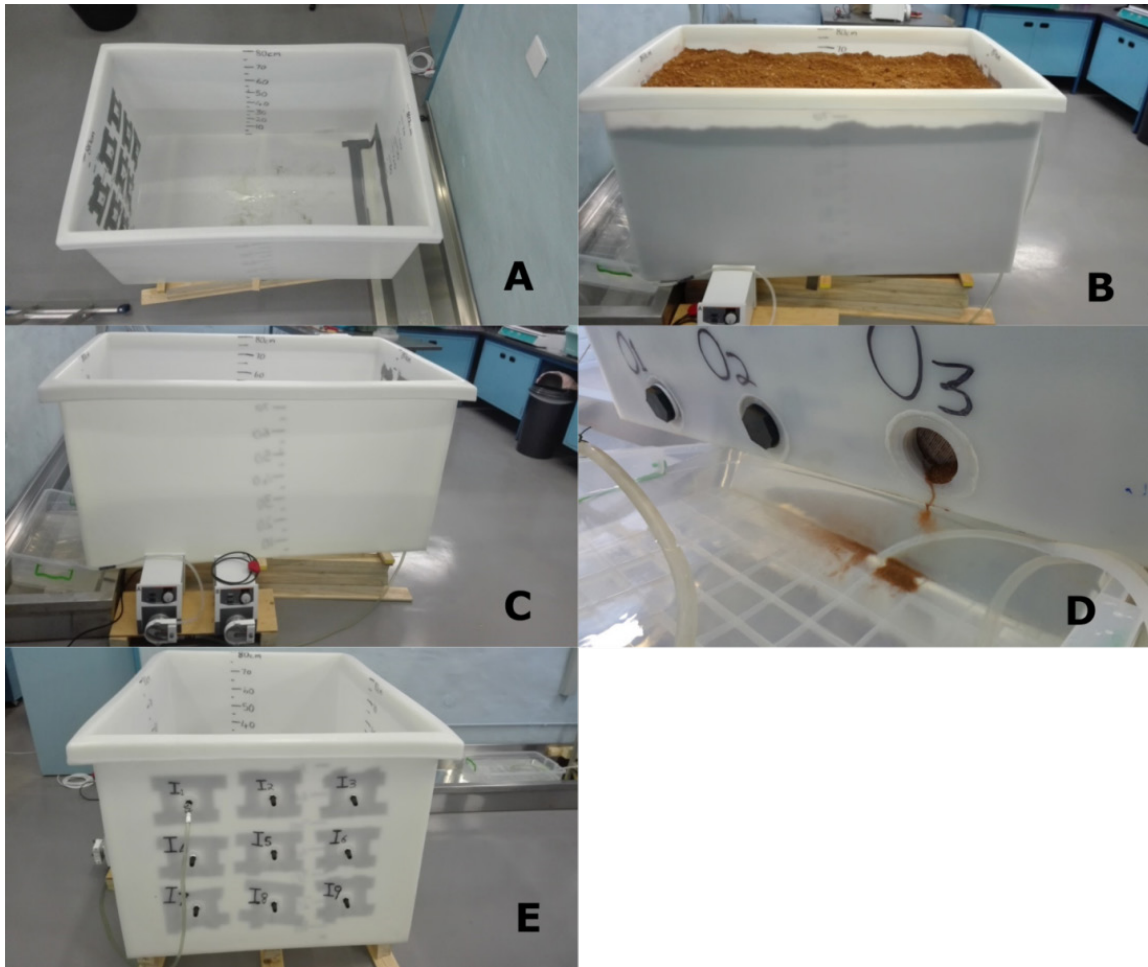


Figure 4.1: Full view of the analogue model. A: showing the upper view and the inside of the tank on which outlets and inlets are seen from the inside covered with sieve, B: tank filled with material, C: showing the pumps used during the experiments, D: showing the outlets from the outer part of the tank, labelled O_1 to O_3 , E: inlets from the outer part of the tank, labelled I_1 to I_9 . Spacing of the marks 10 cm

Based on the results of the 45 sieve analyses, this synthetic material was then composed and mixed in the laboratory (inert quartzitic material; De Souza Hardware & Brick Depot, Akasia, South Africa). From the median values of the sieve analyses, hydraulic conductivities were calculated using the equations of Seelheim and Bialas (Aschenbrenner, 1996) and were found to be around 5.0×10^{-4} m/s ($n = 41$) and 1.8×10^{-5} m/s ($n = 16$) respectively.

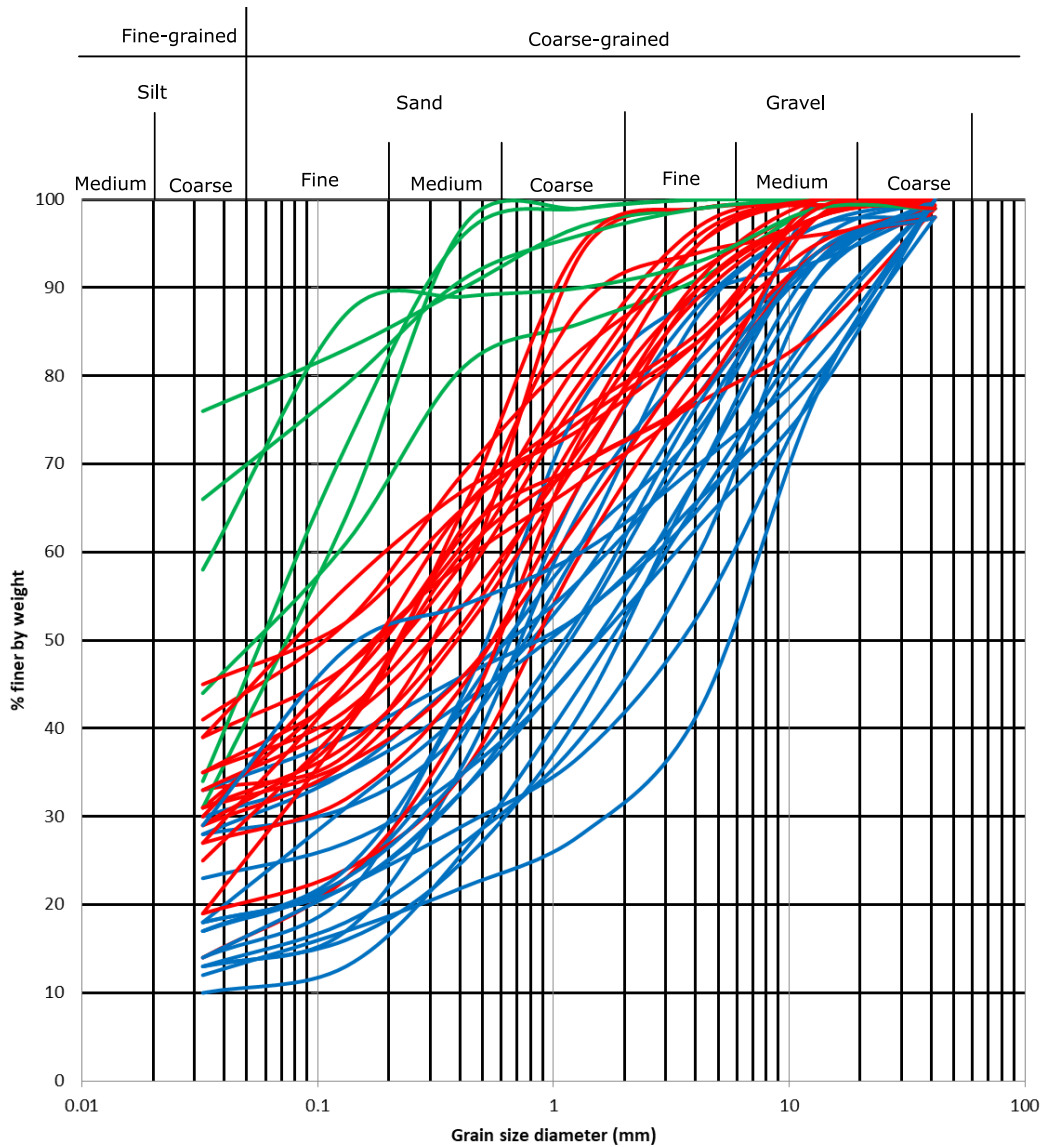


Figure 4.2: Curves for the 45 sieve analyses in Schuch (1981). Green: moraine material, red: fluvial/glaciofluvial sediments and blue: rockslide debris.

Table 4.1: Statistical data of the 45 sieve analyses in Schuch (1981). Std. Dev.: Standard deviation of the population

Material type	Size range, mm	Median	Average	Min.	Max.	Std. Dev.
Silt	0.002 – 0.063	29%	29%	10%	76%	14%
Sand	0.063 – 0.2	7%	10%	3%	38%	8%
Sand	0.2 – 0.63	13%	14%	2%	33%	6%
Sand	0.63 – 2	15%	16%	1%	37%	9%
Gravel	2 – 6.3	15%	14%	1%	27%	7%
Gravel	6.3 – 20	11%	12%	0%	36%	9%
Gravel	20 – 63	2%	5%	0%	22%	7%

Table 4.2: Calculated sediment mass based on the Schuch (1981) data, and real composition of the synthetic rock material used for experiments № 3 and 5. No results are available for experiments № 1, 2 and 4

Material type	Size range, m	Sediment mass, kg %	Experiment 3, %	Experiment 5, %	Average, %
Silt	0.002 – 0.063	481 31	18	11	15
Sand	0.063 – 0.2	116 8	24	18	21
Sand	0.2 – 0.63	215 14	26	16	21
Sand	0.63 – 2	249 16	3	8	6
Gravel	2 – 6.3	249 16	21	34	28
Gravel	6.3 – 20	183 12	4	5	5
Gravel	20 – 63	34 2	3	7	5

A number of parameters were modified during the five experiments. This includes the number of inlets and outlets used, compaction of material and number of pumps used (Table 4.3). This was necessary for understanding the Toma Hill formation mechanism. The changes do not include the type of material, since similar combination of material was used throughout all five experiments.

Table 4.3: Summary of experiments № 1 to 5

	Exp 1	Exp 2	Exp 3	Exp 4	Exp 5A	Exp 5B
Number of pumps used	2 in day 1; 1 from day 2 onwards	2	2	2	2	2
Inflow, L/min	1.1 for O ₂ 0.5 for O ₃	1.2 for O ₂ 0.5 for O ₃	0.9 for O ₂ 0.2 for O ₃	0.8 for O ₂ 0.1 for O ₃	0.8 for O ₂ 0.1 for O ₃	0.7 for O ₂ 0.3 for O ₃
Inlets used	l ₁ & l ₃ . l ₁ was changed for l ₄ and l ₃ for l ₆ on day 1; only l ₄ was used from day 2 onwards.	l ₇ & l ₉ ; on day 15, l ₉ was changed for l ₈	l ₇ & l ₉	l ₇ & l ₉	l ₆ & l ₇ ; on day 2, l ₆ was changed for l ₉	l ₇ & l ₆
Outlets used	O ₂ & O ₃	O ₂ & O ₃	O ₂ & O ₃	O ₂ & O ₃	O ₂ & O ₃	O ₂ & O ₃
Duration	30 days	30 days	32 days	30 days	5 days (not finished)	30 days
Average flow at outlet, mL/min	0.8 for O ₂ 0.3 for O ₃	1.0 for O ₂ 0.4 for O ₃	0.7 for O ₂ 0.1 for O ₃	0.7 for O ₂ 0.2 for O ₃	None experiment interrupted	→ 0.8 for O ₂ 0.4 for O ₃
Remarks	None	Blue aquarium gravel “acting” as moraine	20 cm long pipes extending inlets l ₇ & l ₉ from the inside of the tank	Flow started at the very bottom of the tank. Material was compacted	Same setup as Exp. № 5B; experiment stopped, as wrong material was delivered	20 cm long pipes used to extend inlets l ₇ & l ₆ from the inside of the tank
Material height, cm	69	58	55	50	54	55
Hydraulic gradient	0.33	0.17	0.17	0.17	0.17	0.17

Pump flow rate was adjusted for several times until the correct speed to use was found. The reason to adjust the speed was because of the overflowing tank, i.e. Q_i is greater than Q_f . The Fernpass rockslide area is dominated by glacial activity that took place years ago. Therefore, blue aquarium gravel was used as moraine in experiment 2 to help understand the hills material which contains enough amount of moraine. It was evident that as internal erosion is taking place, cracks form and “moraine” would descend into these cracks and ultimately form part of hills material composition.

Preferential flow of water to the tank’s surface was experienced in experiments № 1 and 2. Therefore, modifications were done in the following 3 experiments to prevent this type of flow. In experiments № 3 and 5, 20 cm long pipes were used to extend inflows from the inside of the tank. In experiment № 4, the pipes were adjusted in such a way that the flow of water started from the very bottom of the tank, and the material was compacted. Preferential flow may have occurred due to the smooth surface of the tank, i.e. the smoothness of the tank on the inside made it easy for water to flow up quickly and pile up on top. However, this type of flow continued throughout the experiments and formed water-filled depressions which can also be found in the Fernpass rockslide area.

4.3 Additional experimental procedures

The objective of the study was to provide a first approach using an analogue lab scale model for investigating internal erosion occurring in sediment that build up Toma Hills. The Fernpass rockslide material comprises a mixture of coarse and fine particles, in which it was expected that the fine grains will be eroded by groundwater flow resulting in internal instability of the rockslide debris.

In the gravel material used in the experiment, the coarse fraction formed a skeleton texture, and it was observed that internal erosion by suffosion transported the smaller fraction of the sediment. During this process, finer material is detached by the action of seepage flow once the water velocity exceeds a given threshold. It is then transported through the voids within the coarse material and redeposited within the interstitial space of the material itself once the velocity falls below a threshold velocity. This, consequently, reduces the porosity. This was observed during the experiments when cracks formed in the analogue model, finer material being eroded, and discharge in the outlets O₂ and O₃ reduced during the experiment, implicating a reduction in porosity. A sample of this eroded finer material during experiments № 4 and 5B was analysed by laser diffraction together with the finer material found in the limnokrene in the Fernpass area near Biberwier.

The following parameters were varied for the analogue modelling of the formation of the Toma Hill: flow, hydraulic gradient and compaction of the material. Precipitation or fluvial processes were not simulated in these experiments, since the tank did not have a drain for running water above ground. The Hjulström diagram (Hjulström, 1935; Sundborg, 1956) and the grain size distribution of the material eroded from the tank were used to estimate the water velocity within the tank (Figure 4.3).

To evaluate the mean residence times and velocities of the water in the analogue model, two tracer tests with sodium chloride (NaCl, table salt) were conducted. As concentrated salt solutions tend to flow to the bottom of the tank, the smallest possible concentrations for obtaining peaks were used and the tap water allowed to reach ambient temperature. A 10 g (33.3 g/L) and 20 g (66.7 g/L) of Na, respectively, were dissolved in 300 mL of tap water and thoroughly stirred on a magnetic stirrer until all the salt was completely dissolved.

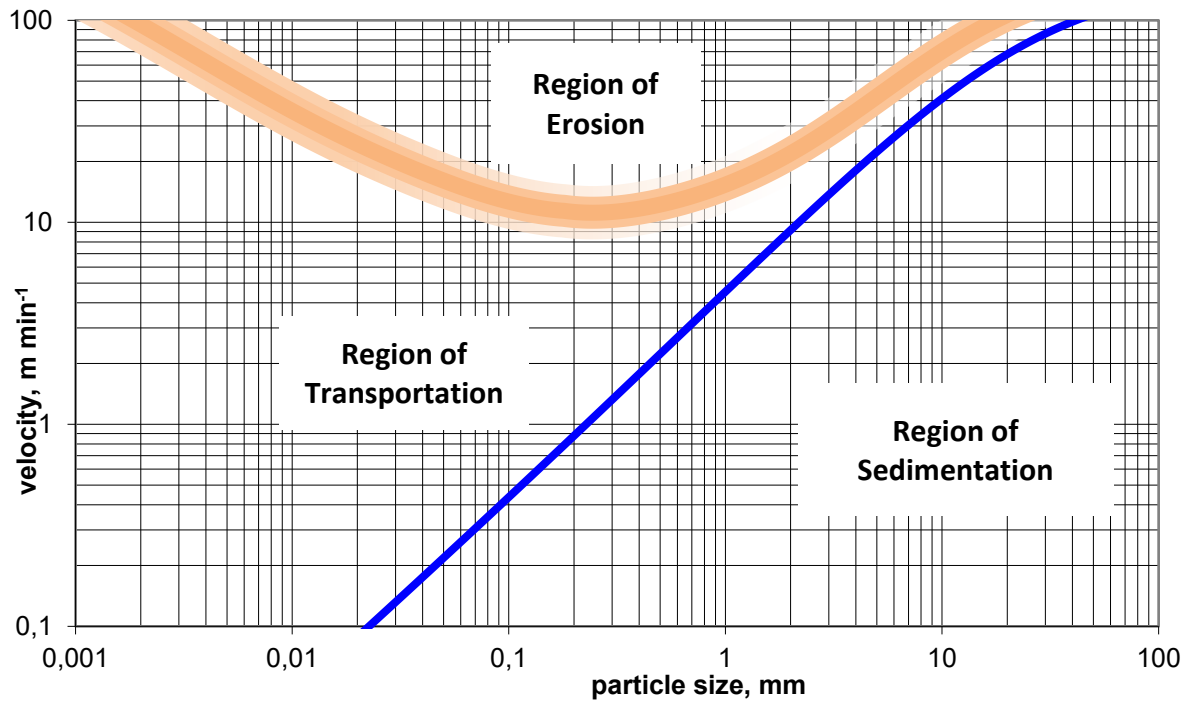


Figure 4.3: The Hjulström diagram modified after Hjulström (1935) and Sundborg (1956)

CHAPTER 5

5 Results and Discussions

5.1 General features observed during the experiments

Five experiments with various boundary conditions were conducted to test the hypothesis of the Toma Hill formation in the analogue model. During all the five experiments, it was evident that internal erosion by suffusion has a substantial influence in the structural formation of the Hills through the formation of cracks, lateral depressions and erosion of finer material. During experiment № 1, a lateral depression occurred on both sides of the tank and it took about 16 days for the water to finally infiltrate into the sediment. Cracks also formed and continued to widen for straight 22 days. Only one inlet was used from day 2 to day 30 of the experiment and this lead to only one limnokrene-like feature developing (Figures 5.1 and 5.2).

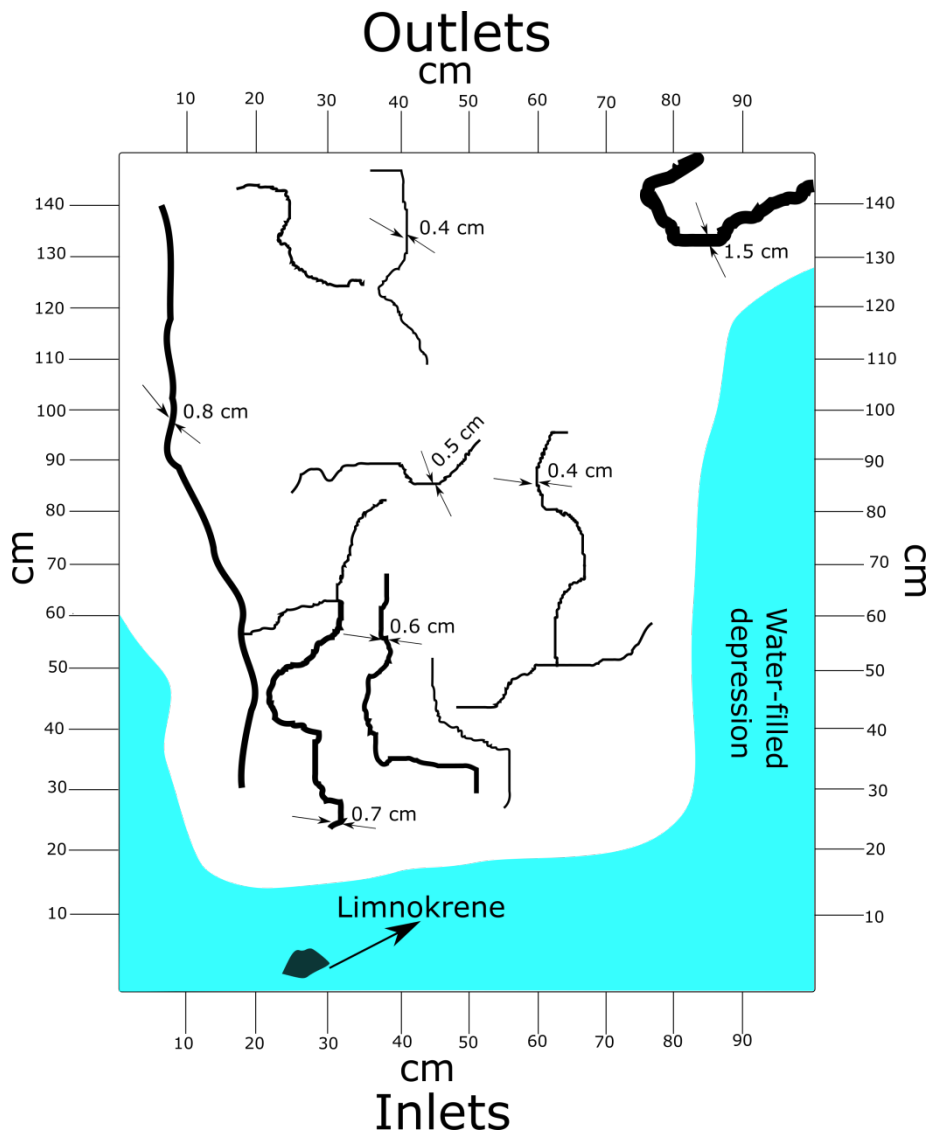


Figure 5.1: A schematic sketch of the features observed during experiment № 1. Centimeter labels inside indicates the width of the cracks developed during the experiment. Also see electronic attachment A using the link www.wolkersdorfer.info/rockslide_more_A.

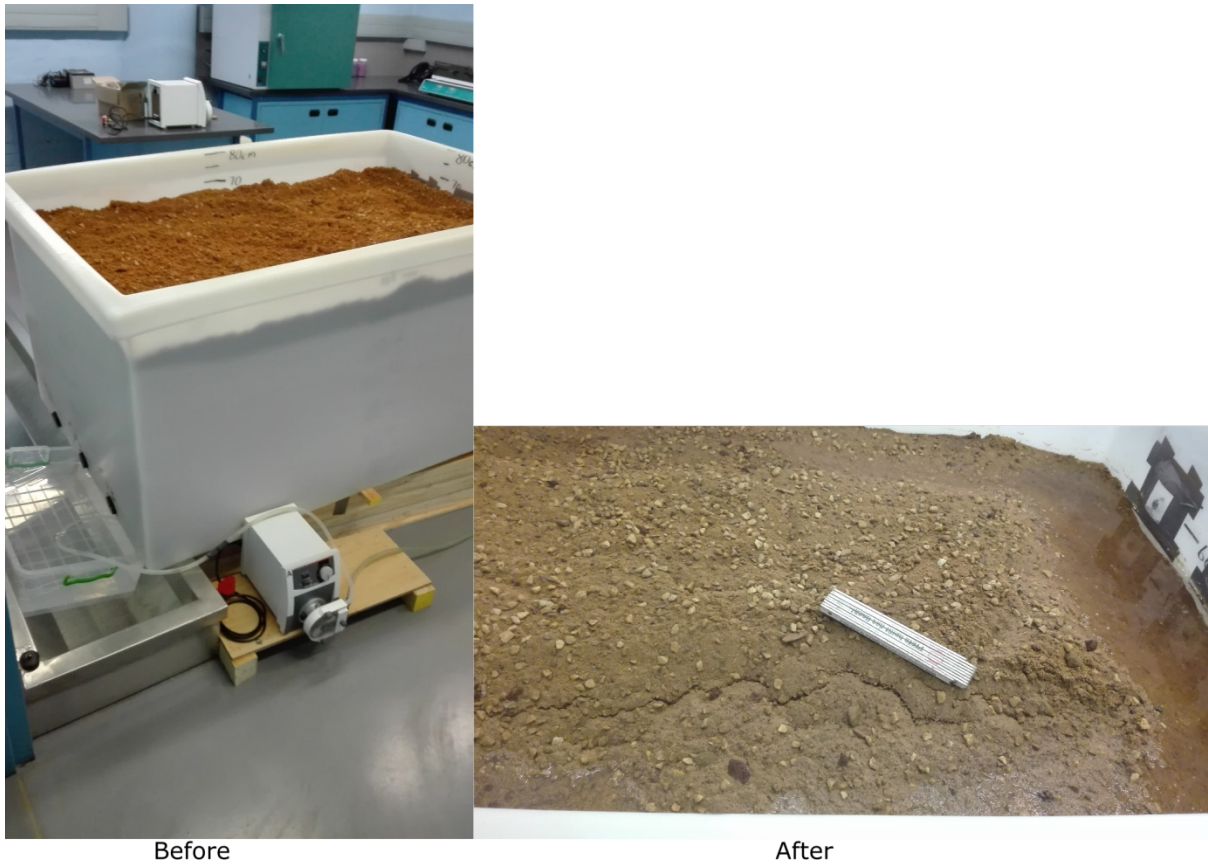


Figure 5.2: Before (left) and after (right) the run of experiment № 1

A maximum of 2 inlets were used in experiment № 2, but only a single feature of limnokrene was observed. The main reason for this may be likely because of preferential flow that occurred during the experiments. Less cracks compared to experiment № 1 cracks developed, and a water trough only formed on one side of the tank (Figures 5.3 and 5.4).

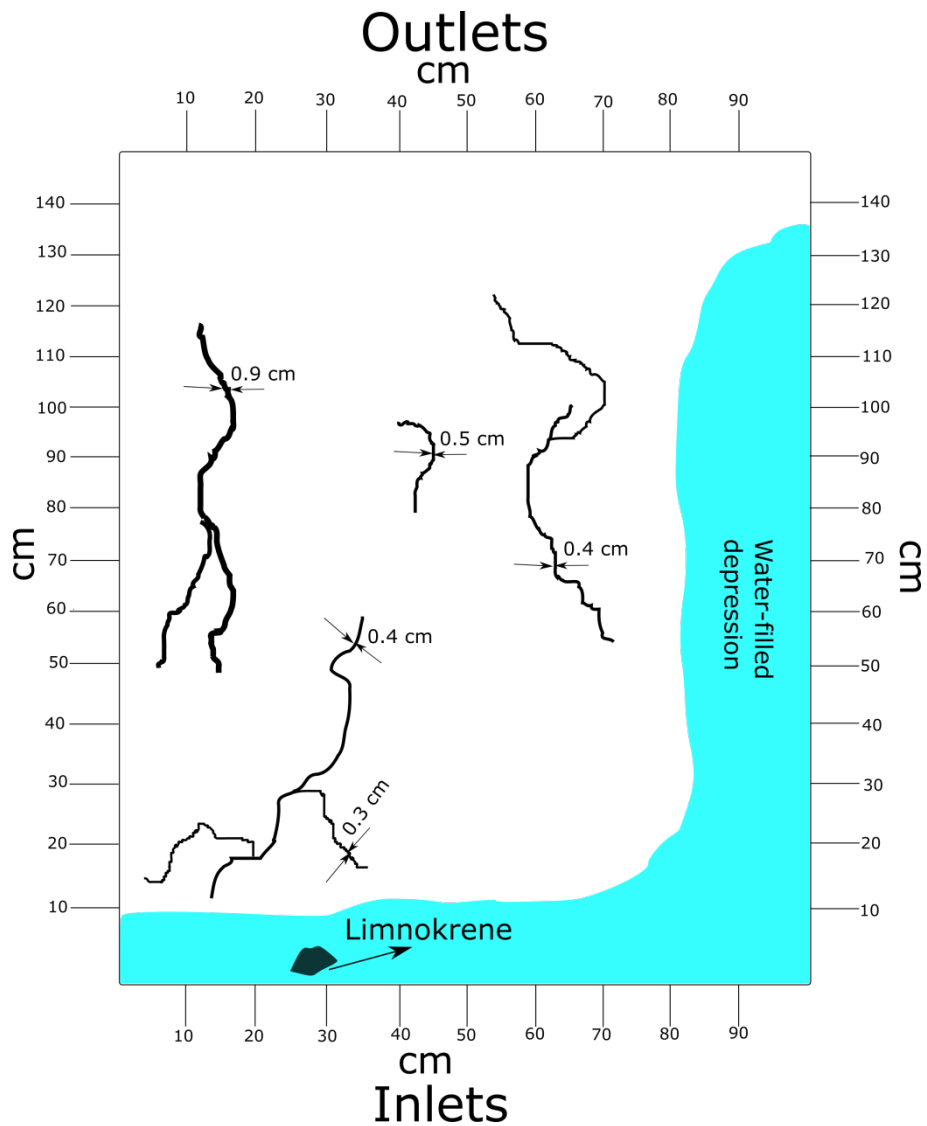


Figure 5.3: A schematic sketch of the features observed during experiment № 2. Centimeter labels inside indicates the width of the cracks developed during the experiment. Also see electronic attachment B using the link www.wolkersdorfer.info/rockslide_more_B.

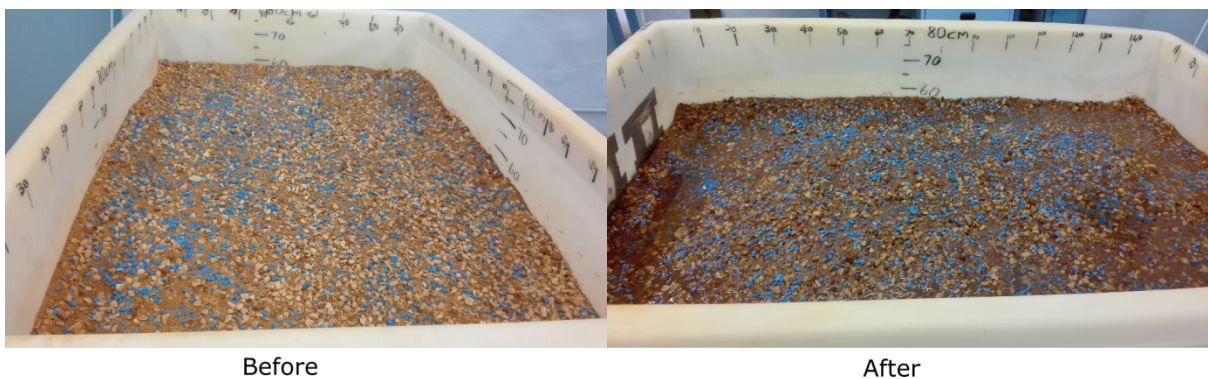


Figure 5.4: Before (left) and after (right) the run of experiment № 2

A trend of decreasing number of visible cracks continued in experiment № 3 in which the number of cracks developed was much less compared to both experiments № 1 and 2. Lateral depressions occurred on both sides of the tank, and two limnokrene features developed. It took 10 days for the cracks to form and they widened from an average width of 0.4 cm to 1 cm for straight 16 days (Figures 5.5 and 5.6).

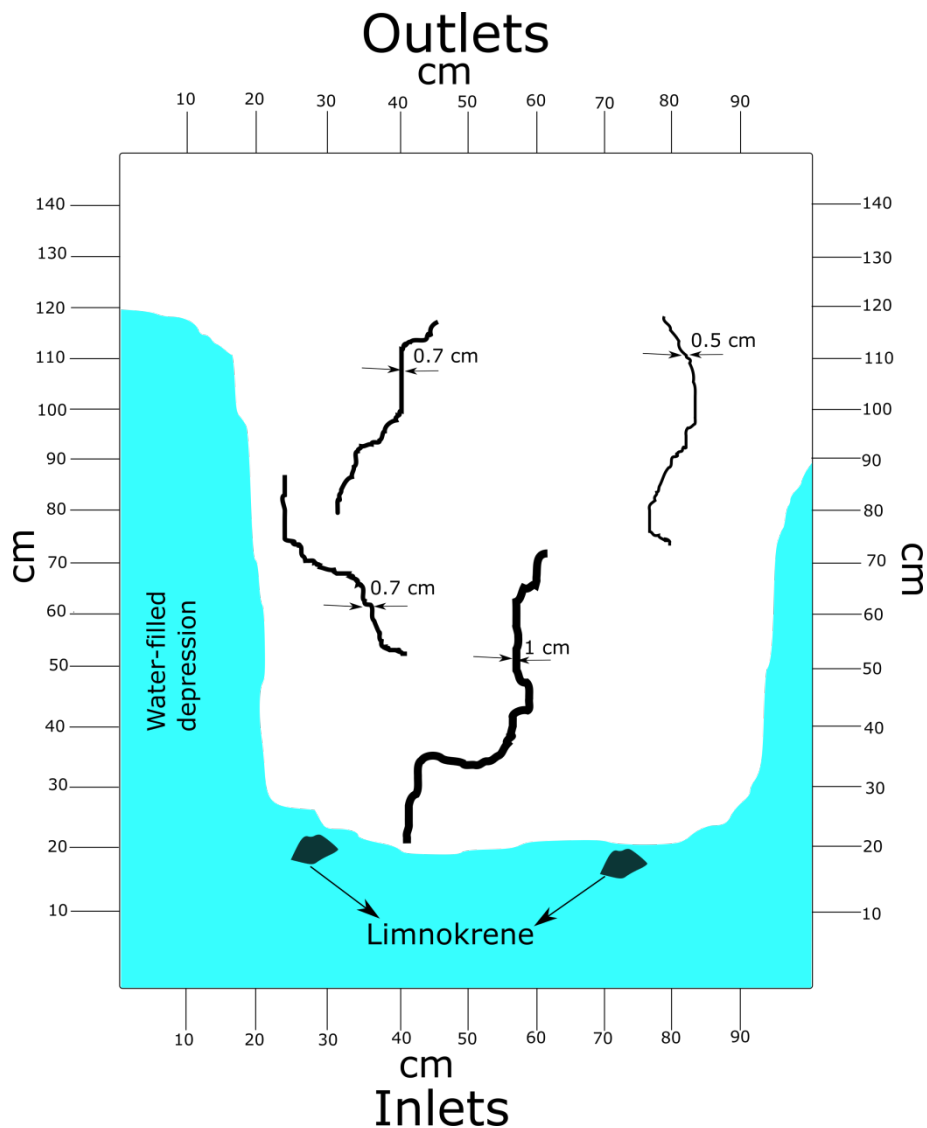


Figure 5.5: A schematic sketch of the features observed during experiment № 3. Centimeter labels inside indicates the width of the cracks developed during the experiment. Also see electronic attachment C using the link www.wolkersdorfer.info/rockslide_more_C.

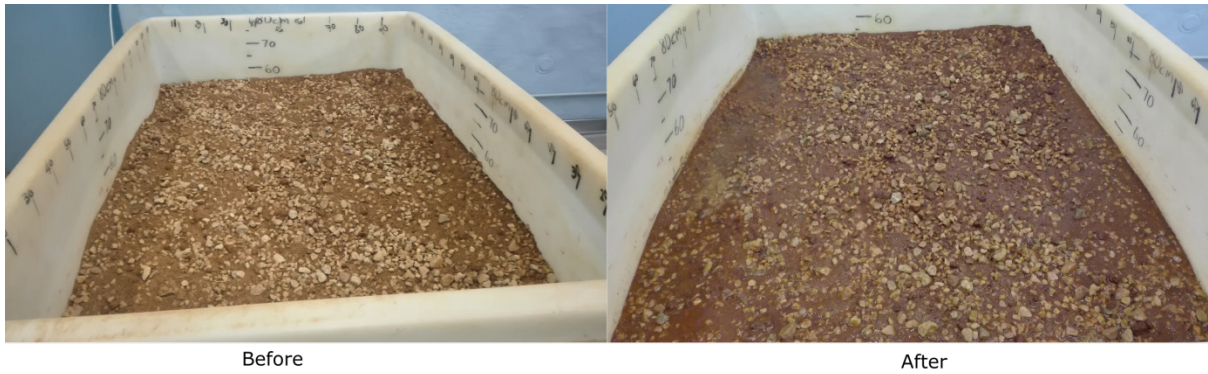


Figure 5.6: Before (left) and after (right) the run of experiment № 3

In experiment № 4, the limnokrene feature was not well developed since “groundwater” flow started from the very bottom and the material was compacted. Modifications of parameters do affect the experiment positively and negatively. A lateral depression was also not well developed, and fewer cracks formed (Figure 5.7 and 5.8).

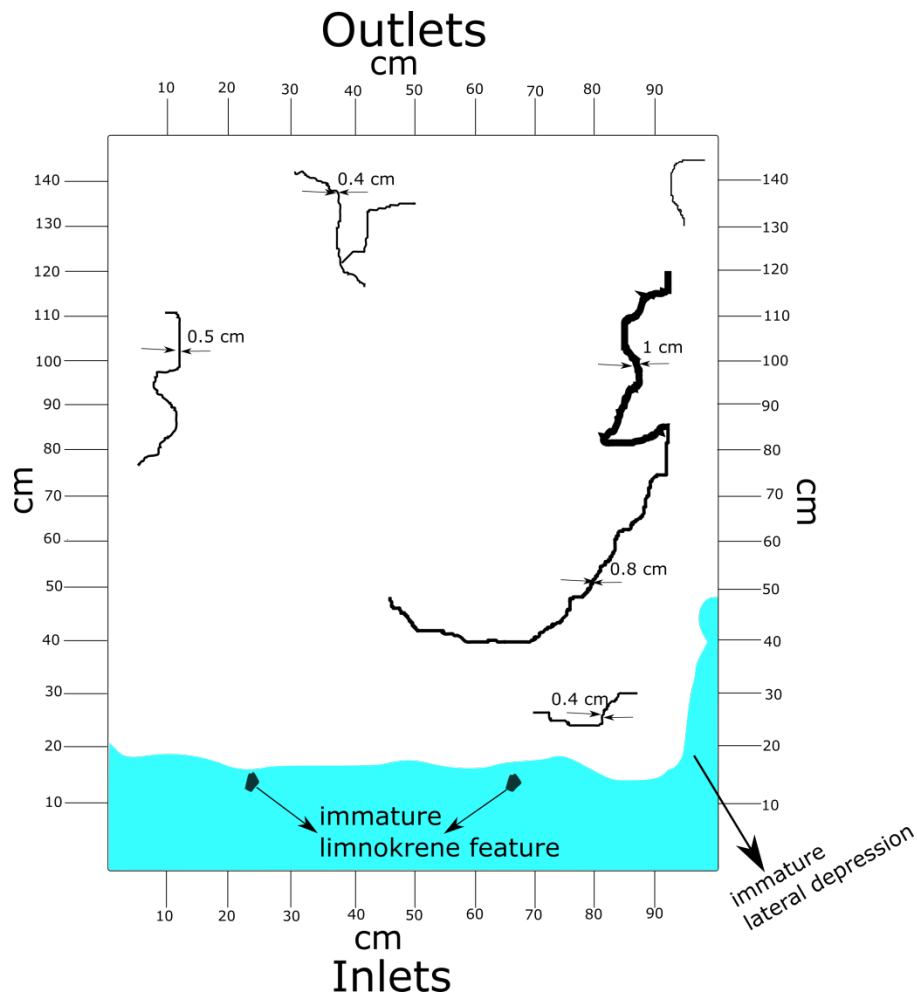


Figure 5.7: A schematic sketch of the features observed during experiment № 4. Centimeter labels inside indicates the width of the cracks developed during the experiment. Also see electronic attachment D using the link www.wolkersdorfer.info/rockslide_more_D.

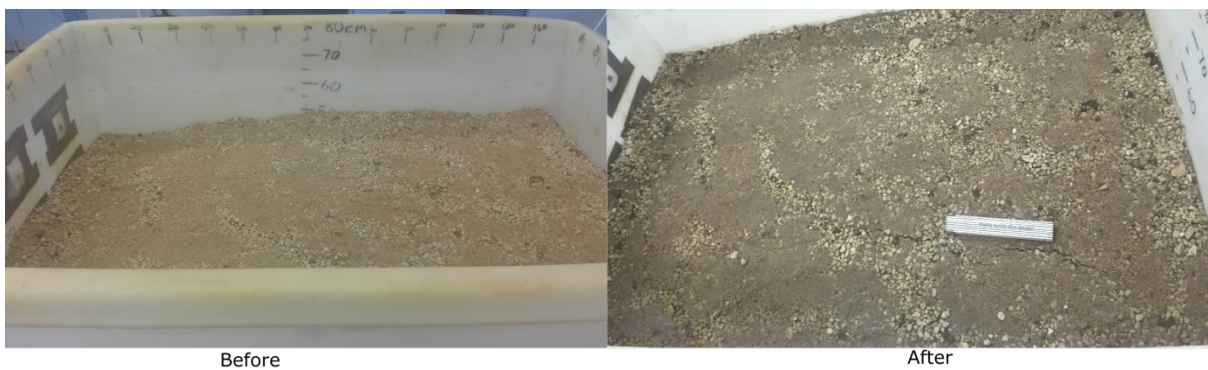


Figure 5.8: Before (left) and after (right) the run of experiment № 4

Experiment № 5A was stopped just after 5 days due to constant overflowing of the water in the tank; therefore, no results were yielded for this experiment. Experiment № 5B showed full development of features, i.e. lateral and transversal cracks, a

limnokrene and lateral depression. A clear structural formation and angles of the hills were observed during the experiment. Cracks developed from day 1 of the experiment and widened for the next 29 days as the experiment ran for 30 days. Finer material was clearly seen to be flowing up from the limnokrene to the surface. Plants formed during the experiment (Figure 5.9 and 5.10).

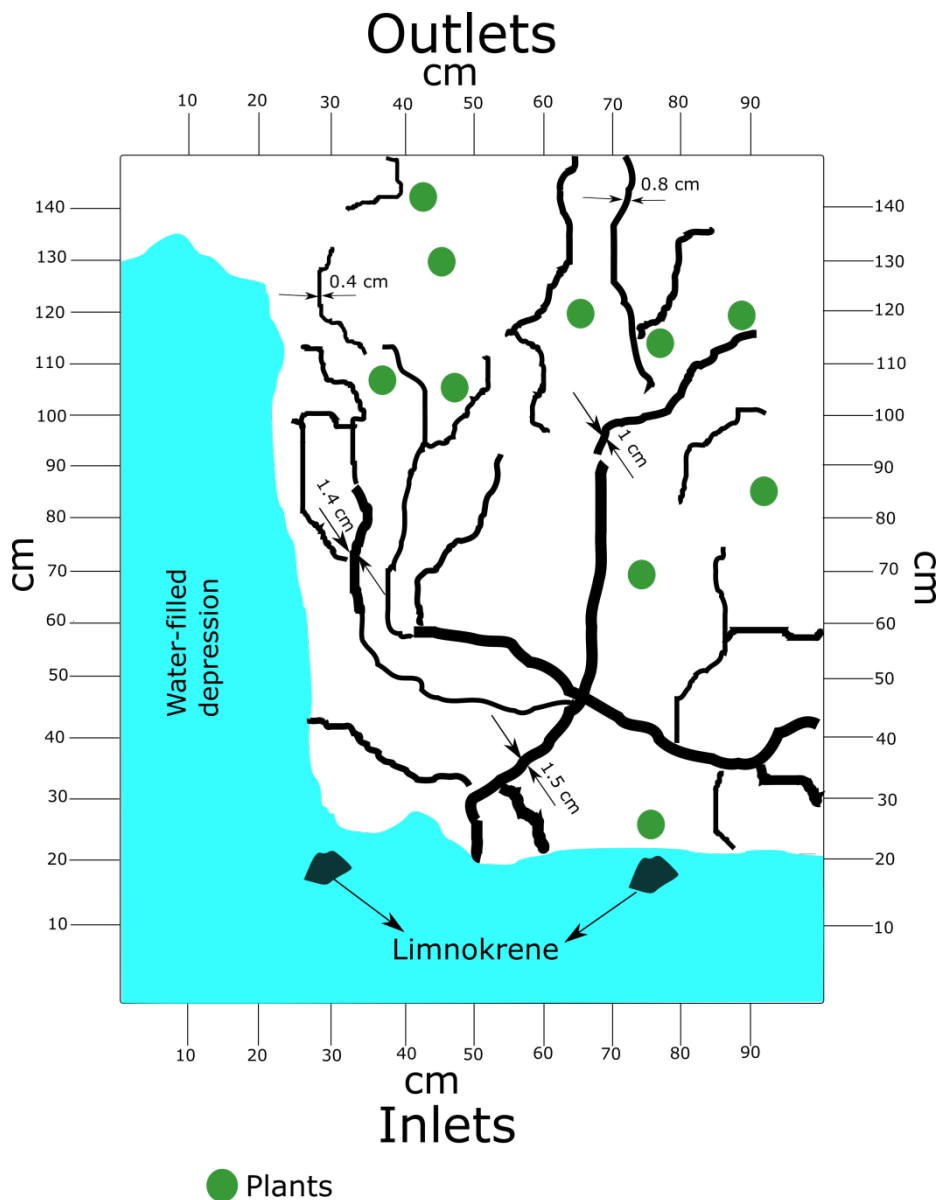


Figure 5.9: A schematic sketch of the features observed during experiment № 5B. Centimeter labels inside indicates the width of the cracks developed during the experiment. Also see electronic attachment E using the link www.wolkersdorfer.info/rockslide_more_E.



Figure 5.10: Before (left) and after (right) the run of experiment № 5B

5.2 Discussion

Internal erosion is a slow process, as groundwater flows slow through the subsurface. As all the five experiments ran for 30 days, with the exception of experiment № 5A that ran for 5 days, with close to natural conditions, only a small amount of material was eroded (on average 136 – 317 g), (Table 5.1). This eroded material has a grain size of at most 0.425 mm and on average a d_{50} of 373 μm . It took a maximum of 4100 years for Toma Hills to form, therefore if this process would have occurred for a longer period of time in the lab, with additional precipitation, the morphology of the Hills would have been clearly seen (electronic attachment www.wolkersdorfer.info/rockslide_more_E). Therefore, with the above mentioned information and utilisation of the Hjulström diagram (Hjulström, 1935; Sundborg, 1956), groundwater velocities of 1 – 20 m/min can then be derived. Using the grain distribution curve, hydraulic conductivities for the synthetic sediment were found to be 2.1×10^{-4} m/s and 8.3×10^{-5} m/s according to Seelheim and Bialas respectively (Aschenbrenner, 1996), and these are slightly lower than the median of the natural material (Table 5.2). During the experiments the outflow was measured frequently and the hydraulic gradient was adjusted, therefore using this together with Darcy's law (Darcy, 1856; Hölting *et al.*, 2013) the hydraulic conductivity was found to be around

8.7×10^{-5} to 8.0×10^{-5} m/s. Schuch (1981) found his hydraulic conductivities determined in the laboratory to be around $a \times 10^{-5}$ to 4.8×10^{-5} m/s, which might be substantially lower than the real ones in the field (Table 5.2). The reason for this maybe that the sieving method of Schuch (1981) results in generally finer sediments than in reality (pers. comm. H. Mostler, 2017). Yet, besides these issues, we found a good agreement between the lab results and the morphological features of the real world situation.

Table 5.1: Mass of the eroded material of the experiments. Experiment 5A was stopped after some days, as material delivered had a too small grain size.

	Exp 1	Exp 2	Exp 3	Exp 4	Exp 5B	Average	Stdev
Eroded material, g	317.0	202.3	158.2	136.8	202.6	203.4	62.3

Table 5.2: The hydraulic conductivity for the material on the northern branch determined by different methods

Method	k_f , m/s
Natural material (calculated)	$1.8 \times 10^{-5} - 5.0 \times 10^{-4}$
Synthetic material (calculated)	$8.3 \times 10^{-6} - 2.1 \times 10^{-4}$
From experiment (measured)	$8.7 \times 10^{-6} - 8.0 \times 10^{-5}$
Schuch (1981)	$a \times 10^{-5} - 4.8 \times 10^{-3}$
Wolkersdorfer (unpublished field data)	$8.1 \times 10^{-7} - 1.1 \times 10^{-6}$

Lateral and transversal cracks formed in all experiments within few minutes after the water inflow was started (Figure 5.11). These cracks implicate substantial contribution of internal erosion by suffosion. During the experiment, all the cracks began to widen; for experiments № 1 and 5 they widened to a width of about 2 cm and for experiments № 2, 3 and 4 about 0.5 – 1 cm of widening was observed. On the sides of the tank, lateral depressions with a width of about 5 – 13 cm and a depth just about 2 – 3 cm developed in all five experiments (Figure 5.11). Water began to accumulate in these

depressions over time and after a couple of days they would sometimes disappear (by infiltration into the “underground”). This observation is interesting in so far, as it mirrors the formation of the more or less lateral Blindsee and Weißensee lakes in the northern branch of the Fernpass rockslide. It can be assumed that the internal erosion of rockslide material on the flanks of the debris was larger than in the middle, causing a preferential lake formation there.



Figure 5.11: Beginning of the formation of cracks and a water-filled depression during experiment № 1. Spacing of the marks 10 cm (photographer: More KS)

In experiment № 4, the material was compacted during tank filling; however, all the features that occurred in the uncompacted experiments developed similarly; i.e. lateral and transversal cracks as well as lateral depressions. When cracks crossed each other, sometimes isolated “hills” appeared in those cases, where the material’s characteristic slope angles allowed their formation during the course of the experiment (Figure 5.12).

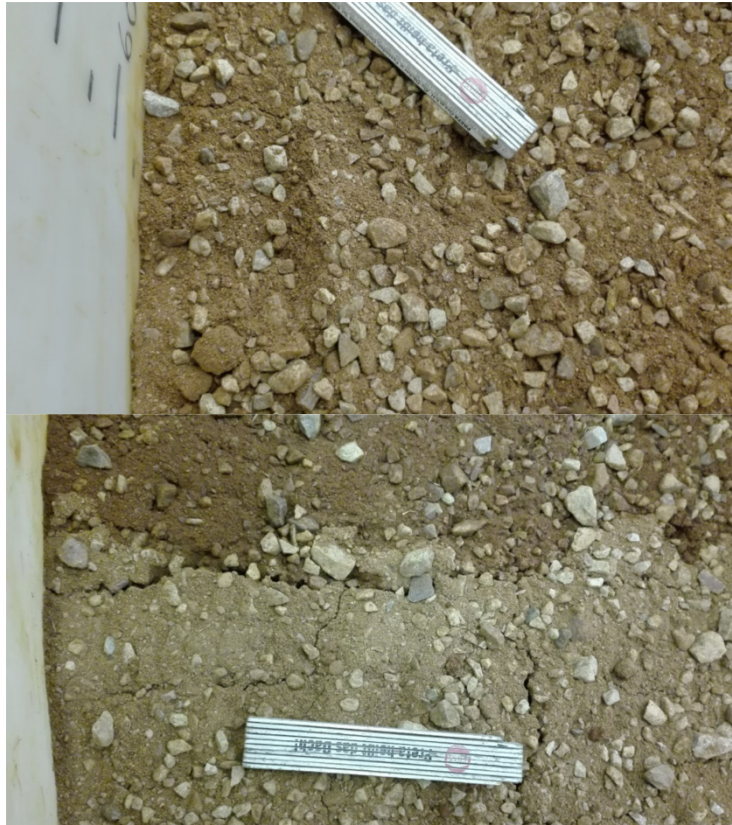


Figure 5.12: Formation of isolated Hills as cracks crossed during experiment № 5. Spacing of the marks 10 cm

Another feature that developed in all the experiments was a limnokrene (sensu Bornhauser, 1912; also written limnocrene), which is the emergence of an aquifer in a basin. In the experiments, these limnokrenes formed on the inlet side, where water was introduced into the tank (Figure 5.13). A similar limnokrene exists south-west of Biberwier, about 20 m east of the Pastor Fink Trail. It has the same characteristics as those observed during the experiments, with finer sediments swirling where the groundwater emerges to the surface.

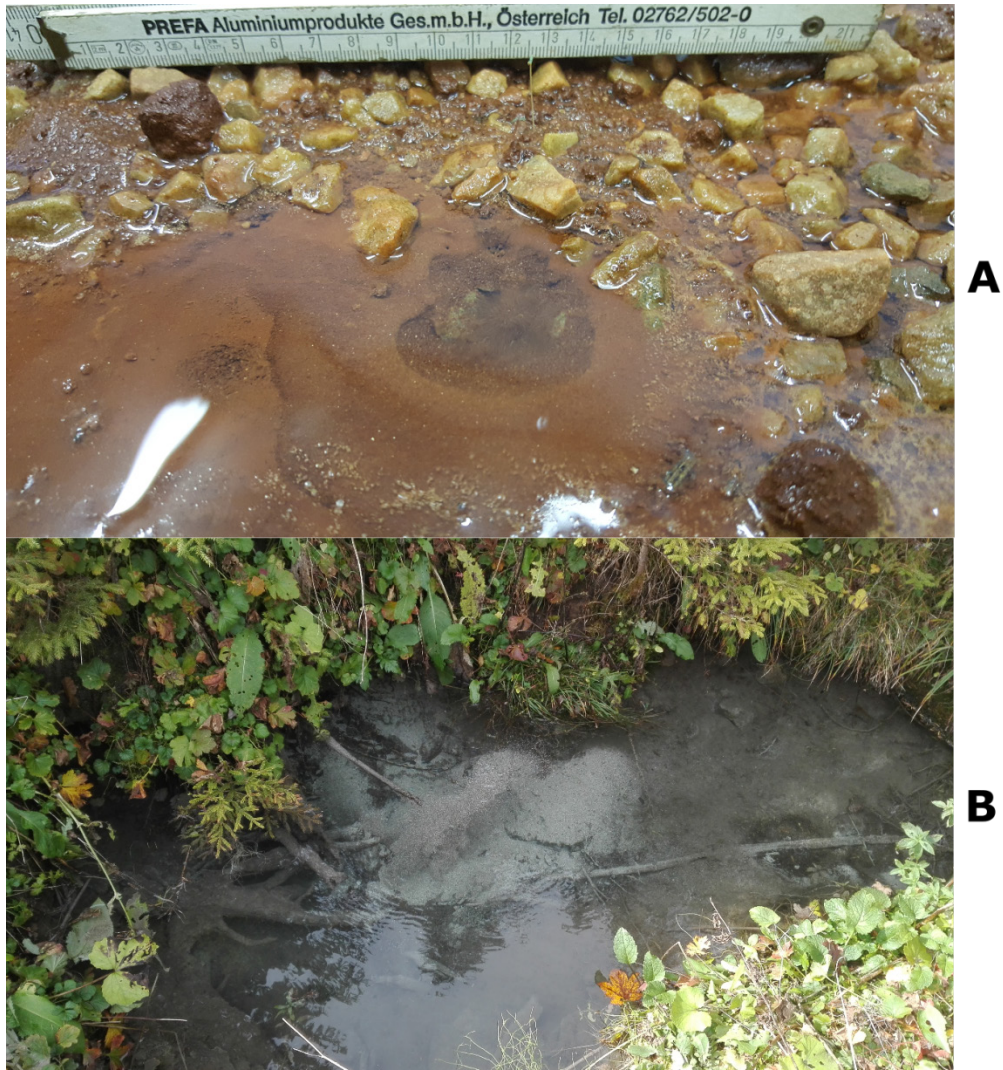


Figure 5.13: Development of limnokrene; A: limnokrene developing during experiment № 3 (photographer: Ch. Wolkersdorfer), B: limnokrene at the Fernpass near Biberwier. Width of image is 2 m (photographer: K.S. More)

5.3 Description of the eroded and lateral depression of material

During the experiment, finer material was eroded daily at a varying rate, implying that internal erosion is taking place. At the same time, also the volume of the combined mixture of silt, sand and gravel in the tank reduced by about 0.08 – 0.2 m³, and therefore, according to the definitions of Fannin *et al.* (2014), internal instability resulting from suffosion occurred (Figure 5.14).

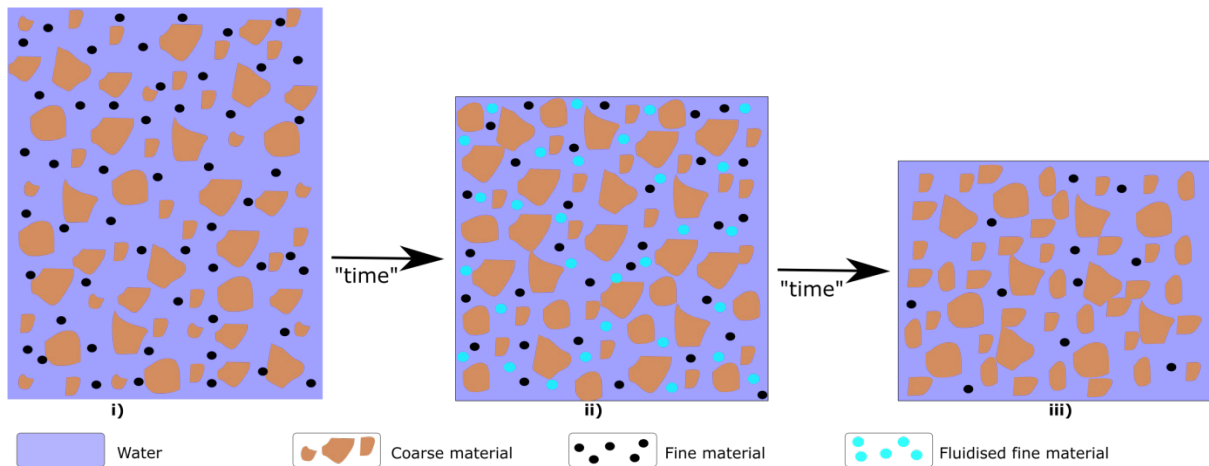


Figure 5.14: The process of suffusion; i) intact material, ii) internal erosion taking place, iii) material after full internal erosion occurred

The process of grain detachment due to seepage flow is controlled by different parameters such as the velocity of flowing water, hydraulic gradient, porosity, the concentration of fluidised material and the amount of material that can be eroded (Figure 5.14). During each single experiment, the hydraulic gradient was kept constant and the inflow speed varied which influenced the change in groundwater flow velocity and ultimately influencing porosity. The amount of finer material being eroded reduced during the continuation of each experiment and lateral depressions developed (Figure 5.15), implicating varying flow velocity and porosity.



Figure 5.15: Development of lateral depression during experiment № 1. Spacing of the marks 10 cm (photographer: K.S. More)

5.4 Sieve analysis and laser diffraction

In order to compare experiment material behaviour and characteristics that took place during the experiment with material of the Fernpass rockslide area, a gradation test was performed in two of the experiments: experiments № 3 and 5. In addition to this, a laser diffraction analysis was also performed on the eroded material. These analyses are used to determine aggregate particle size distribution. For the gradation test, three samples of around 20 kg were taken at three random places in the tank after a successful completion of the experiment. Laser diffraction samples were also taken after the full run of experiment № 4 and 5.

From the results obtained for the gradation test, a graph was produced to compare the results to those of Schuch (1981). Based on experiment № 3 and 5 results, the grain sediment had a grain size of at most 0.425 mm and a d₅₀ of 0.162 mm and 0.719 mm (Figure 5.16) for experiment № 3 and 5, respectively. The hydraulic conductivity based on Bialas and Seelheim calculations (Aschenbrenner, 1996) was 8.55×10^{-6} and 9.4×10^{-5} for experiment number 3 and 1.55×10^{-5} and 2.03×10^{-3} for experiment № 5. This is in range with the hydraulic conductivities for the material in the northern branch which is around $a \times 10^{-5}$ to 4.8×10^{-5} (Schuch, 1981, Table 5.2).

The limnokrene material is one of many examples where finer material of the Biberwier Fernpass rockslide emerges to surface. According to the results obtained (Table 5.3), the coefficient of curvature (C_c) is below 3 for all samples and the uniformity coefficient (C_u) for the Biberwier limnokrene material is less than 3, which means that the sediment is well-graded, uniform and has a very narrow particle size range; that of experiment № 4 and 5B is greater than 5, indicating a well-graded sediment, which has a wide range particle size distribution (Das *et al.*, 2013; Handy *et al.*, 2007; Murthy, 2002). The effective size of the materials (d_{10}), indicates how different the materials

are even though the initial thought in the field was that they are similar. In addition, the d_{50} of the Biberwier limnokrene is twice as large than the eroded material of the analogue experiment (Figure 5.17). The reason for all of the above is that the finer material of the Biberwier limnokrene has already been washed out over the course of time, while the eroded material is the freshly eroded sediment of the experimental setup.

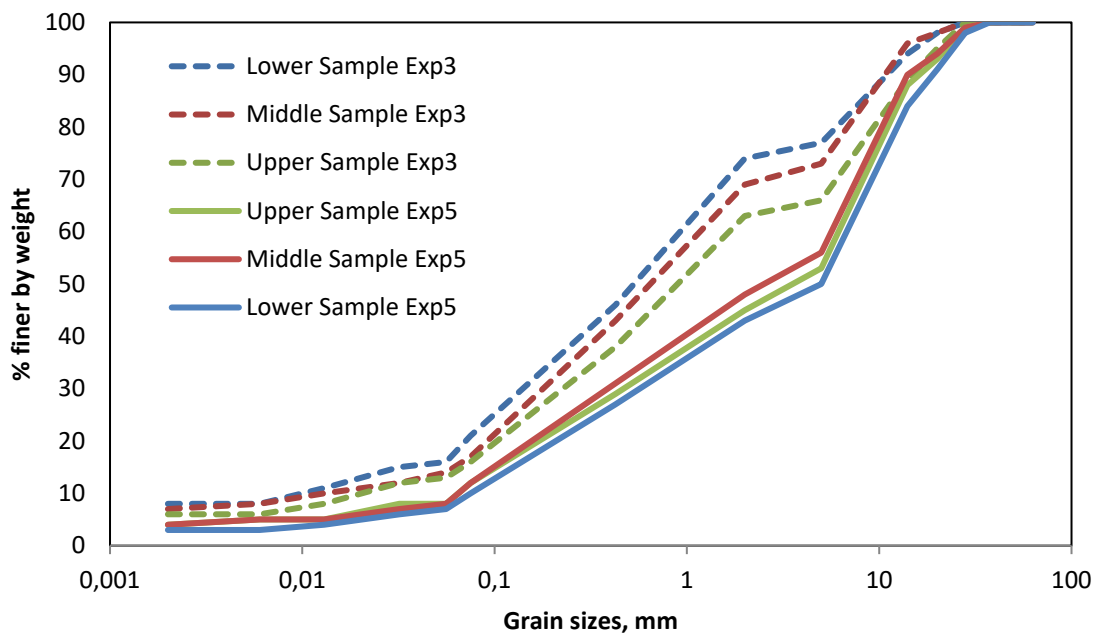


Figure 5.16: Experiments № 3 & 5 gradation curves of the sediments

Table 5.3: Summary of sedimentological parameters of the Biberwier limnokrene material, and eroded finer material of experiments № 4 and 5B; C_u : uniformity coefficient, C_c : coefficient of curvature

Sediment	$d_{10}, \mu\text{m}$	$d_{30}, \mu\text{m}$	$d_{50}, \mu\text{m}$	$d_{60}, \mu\text{m}$	$d_{90}, \mu\text{m}$	C_u	C_c
Limnokrene	421	660	806	970	1584	2.3	1.1
Exp. № 4	76	240	463	586	1250	7.7	1.3
Exp. № 5B	53	165	282	350	680	6.6	1.5

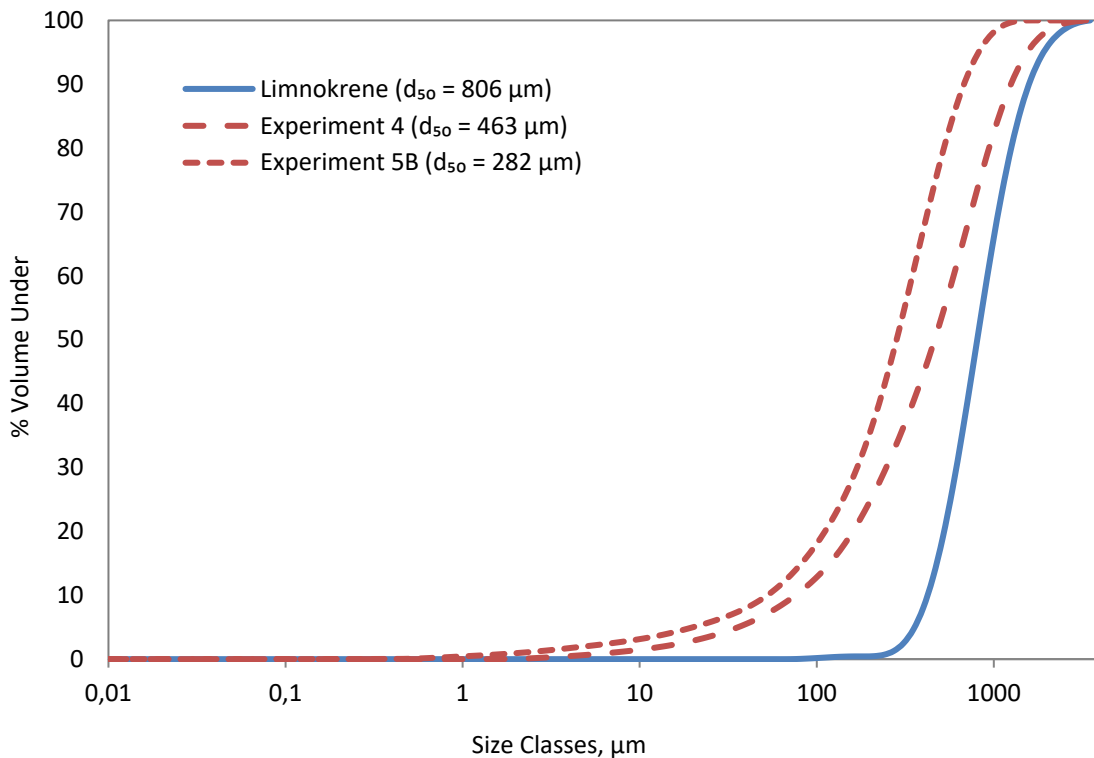


Figure 5.17: Laser diffraction results for the limnokrene material near Biberwier and experiments № 4 and 5B eroded finer material

5.5 Tracer test

A tracer test was performed during experiment № 5. This was conducted in order to understand “groundwater” movement in the tank. Sodium chloride was used as a tracer in this study because it dissolves into cations and anions that increases the ion mobility and thus leading to an increased electrical conductivity (Domenico *et al.*, 1998; Kass *et al.*, 1998). Sodium chloride is widely used in tracer tests as it is nontoxic and has less potential of sorption (Domenico *et al.*, 1998; Kass *et al.*, 1998; Wolkersdorfer, 2008).

A maximum of two tracer tests were conducted; however, the first test did not produce quality results as it was not properly constructed. With reference to the first attempt of the tracer testing, it was observed that 10 g of NaCl solution does not produce a quality

peak. Therefore, 20 g of NaCl solution was used during the second test. Sodium chloride was mixed with 300 mL of Ca-Mg-HCO₃ type, Pretoria tap water. Electrical conductivity (EC) probe A was connected to outlet O₂ of the tank and the EC probe B to outlet O₃ (Figure 5.18). NaCl solution was injected on inlet I₆, and the injection duration was 39 seconds. The tracer test was conducted for 46 hours.



Figure 5.18: Tracer test setup during experiment № 5B, probes in the beakers placed adjacent to the outlets to measure the electrical conductivity

A dispersion type of flow was observed during the test due to the tracer staying for a long time in the system. Dispersion flow is characterised by the flow where one phase is dispersed in the other continuous phase (Domenico *et al.*, 1998; Kass *et al.*, 1998). It was also observed that “groundwater” in the tank flows in a confined manner and not through the whole system. The reason for the resulting tracer shape (Figure 5.19) is because of the cation exchange of the Na⁺ from NaCl tracer solution replacing Ca²⁺ from Ca-Mg-HCO₃ type, Pretoria tap water and thus the electrical conductivity decreased below the base line EC (Kass *et al.*, 1998; Wolkersdorfer, 2008).

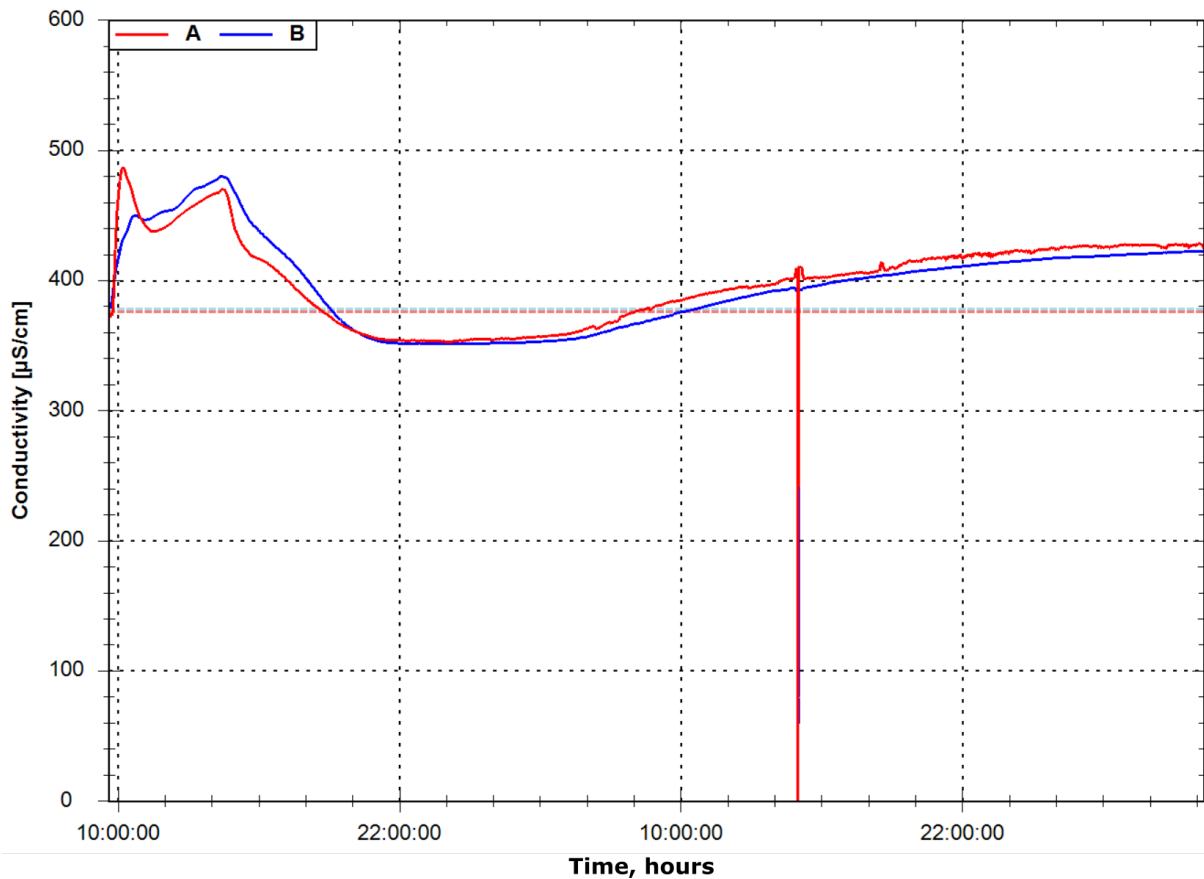


Figure 5.19: EC measurement during tracer test in experiment № 5B. A: indicates probe A measuring EC in outlet O₂, and B: indicates probe B measuring EC in outlet O₃. Peak at between 14:00 and 16:00 on the second day due to emptying the 60 L receiving container

The total quantity of tracer recovered was 20.289 g and the recovery rate of tracer injection was 101.4%, which indicates a good quality of the results obtained. It therefore means that the hydraulic connectivity between the point of injection and point of discharge was good. The first EC peak appeared after 51 minutes and another one after 5 hours. As can be seen from the tracer test result, especially the two peaks, a flow path through the sediment prevail and dispersive flow occurs.

CHAPTER 6

6 Conclusion and Recommendations

As the results show, the analogue Toma hills laboratory model leads to the formation of cracks, depressions and water-filled troughs. This is on the one hand due to materialization, on the other hand due to internal erosion by suffusion of the synthetic rockslide material. At the edges of the analogue model, lake-like structures were formed, in which either water flowed or accumulated. These structures are also found in the Fernpass area, where, for example, the Dorfbach in Biberwier or the Weißensee are present in a similar spatial context. Lateral and transversal cracks, as they developed in the model, are also found on the long-distance pass itself. These have so far mainly been explained by sackings; however, based on the available results from analogue modeling, it must be assumed that these could also have been caused by settlements resulting from internal erosion. Almost all analogue models showed a crack pattern, as can be observed in the topographically higher part of the crest. In addition, the features clearly showed how “hills” similar to those of the Toma hills formed, which allows the conclusion that internal erosion contributes to their formation.

The Fernpass rockslide area is dominated by dolines, and such doline-like structures developed during the experiments. It was previously said that the dolines of the Fernpass are caused by dissolution of gypsum (Mostler, 2013), however the structures were completely explained by the process of internal erosion by suffusion during the experiments, and consequently some of the doline-like structures at the Fernpass might have resulted from this process.

In all of the experiments a limnokrene developed, similar to the one south of Biberwier, but different from the other sources in the northern part of the study area. This indicates that groundwater flows in the subsoil and comes to the surface on preferential flow paths with a lower hydraulic conductivity as a source and transports fine-grained material.

From the results, the formation of the narrow valleys between some Toma hills whose flanks correspond to the natural bed angle of this material can be explained. This could also be shown in the experiment. There, internal erosion resulted in a material deficit and consequently a slipping of the material.

On the basis of the experimental results, the site survey and literature investigations, the morphology of the Toma hills can be explained as follows: rockslide material falls onto and spreads on saturated fluvial sediments, resulting in larger or smaller accumulations of more or less cohesive material. After the rockslide came to its "halt", surface and groundwater started to percolate through the rockslide material, leading to internal erosion, material accumulation and the formation of valleys. Slipping of the material after the valleys formed moved material from the top into the flanks, which would explain the presence of moraine material both at the top of the hills and in their flanks. Through the combination of these processes, the morphology of the Toma hills including a potential syn-genetic rockslide predetermination can be interpreted completely.

It could be of interest to model the fluvial activity of the pre- and post-Fernpass rockslide conditions. This is because during this study it was proven that fluvial activity does indeed contribute in forming Toma hills, and up to this date there is no known work of stream flows in this area before and after the occurrence of the Fernpass

rockslide. It might therefore be of interest that river Loisach existed and that it could have contributed to the rockslide and Toma hills formation per se.

CHAPTER 7

7 References

ABELE, G. 1964. Die Fernpaßtalung und ihre morphologischen Probleme. *Tübinger Geomorphol. Studien*, 12:1-123.

ABELE, G. 1969. Vom Eis geformte Bergsturzlandschaften: zur Frage der glazialen Umgestaltung der Bergstürze von Sierre, Flims, Ems und vom Fernpass. *Geomorphol.*(8):119-147.

ABELE, G. 1974. Bergstürze in den Alpen. Ihre Verbreitung, Morphologie und Folgeerscheinungen. *Wiss. Alpenvereinshefte*, 25:309-324.

ABELE, G. 1991. Der Fernpaßbergsturz-Eine differentielle Felsgleitung. *Österr. Geograph. Ges.*(4):22-32.

ABELE, G. 1994. Large rockslides: Their causes and movement on internal sliding planes. *Mount. Res. & Development*, 14:315-320.

ABELE, G. 1997. Rockslide movement supported by the mobilization of groundwater-saturated valley floor sediments. *Geomorphol.*, 41:1-20.

AMPFERER, O. 1904. Die Bergstürze am Eingang des Ötztales und am Fernpaß. *Verh. k.-k. geol. R.-A.*:73-87.

AMPFERER, O. 1941. *Bergzerreibungen im Inntalraume*. Vienna: Hölder-Pichler-Tempsky.

ARANBURU, A., ARRIOLABENGOA, M., IRIARTE, E., GIRALT, S., YUSTA, I., MARTÍNEZ-PILLADO, V., DEL VAL, M., MORENO, J. & JIMÉNEZ-SÁNCHEZ, M. 2015. Karst landscape evolution in the littoral area of the Bay of Biscay (north Iberian Peninsula). *Quaternary Int.*, 364:217-230.

ASCHENBRENNER, O. 1996. Die Auswertung von Kornverteilungskurven zur Ermittlung der Durchlässigkeit. *Gießener Geol. Schr.*, 56:33-48.

BALTZER, A. 1874/75. Ueber Bergstürze in den Alpen. *Jahrbuch S. A. C.*, 10:409-465.

BORNHAUSER, K. 1912. *Die Tierwelt der Quellen in der Umgebung Basels*. *Int. Rev. Gesamten Hydrobiol. Hydrogr. – Biol. Suppl. V. Serie*, 1-90.

BOX, G.E.P. 1979. *Robustness in the strategy of scientific model building*. New York: Academic Press. (Robustness in Statistics).

BRUNNER, H. 1962. Die Churer Toma. – Bündner Jb. 4:67-75.

CALHOUN, N.C. 2015. LiDAR and geomorphic characterisation of landslide-induced liquefaction deposits in the eastern Swiss Alps. Simon Fraser University.

CAPRA, L. 2011. Volcanic natural dams associated with sector collapses: textural and sedimentological constraints on their stability. In: Evans S., H.R., Strom A., Scarascia-Mugnozza G. (ed.). *Natural and Artificial Rockslide Dams*. Berlin, Heidelberg: Springer: 279-294.

CROSTA, G.B. & CLAGUE, J.J. 2009. Dating, triggering, modelling, and hazard assessment of large landslides. *Geomorphol.*, 103(1):1-4.

DARCY, H. 1856. Les fontaines publique de la ville de Dijon. *Dalmont, Paris*, 647.

DAS, B.M. & SOBHAN, K. 2013. *Principles of geotechnical engineering*. Cengage Learning.

DELINÉ, P., HEWITT, K., REZNICHENKO, N. & SHUGAR, D. 2015. Rock avalanches onto glaciers. In: Davies, T. (ed.). *Landslides Hazards, Risks and Disasters*. Amsterdam: Elsevier: 263-319.

DOMENICO, P.A. & SCHWARTZ, F.W. 1998. *Physical and chemical hydrogeology*. Wiley New York.

DUFRESNE, A. 2014. An overview of rock avalanche-substrate interactions. In: Sassa K., C.P., Yin Y., (ed.). *Landslide Science for a Safer Geoenvironment*. Cham: Springer: 345-349.

DUFRESNE, A. & DAVIES, T.R. 2009. Longitudinal ridges in mass movement deposits. *Geomorphol.*, 105(3-4):171-181.

DUFRESNE, A., PRAGER, C. & BÖSMEIER, A. 2015a. Insights into rock avalanche emplacement processes from detailed morpho-lithological studies of the Tschirgant deposit (Tyrol, Austria). *Earth Surf. Process. Landforms*, 1:1-16.

DUFRESNE, A., PRAGER, C. & CLAGUE, J.J. 2015b. Complex interactions of rock avalanche emplacement with fluvial sediments: field structures at the Tschirgant deposit, Austria. In: Lollino G. (ed.). *Eng. Geol. for Soc. & Territory*. Vol. 2. Cham, Switzerland: 1707-1711.

ERISMANN, T.H. & ABELE, G. 2013. *Dynamics of rockslides and rockfalls*. Heidelberg: Springer.

FANNIN, R. & SLANGEN, P. 2014. On the distinct phenomena of suffusion and suffosion. *Géotechnique Letters*, 4(4):289-294.

GINER, P.J., PION, G. & HORTELANO, L. 2015. Experimental basis in lithic arrows usage and hafting at the end of the last glaciation in the French Alps. *Quaternary Int.*:1-13.

GRAMIGER, L.M., MOORE, J.R., VOCKENHUBER, C., AARON, J., HAJDAS, I. & IVY-OCHS, S. 2016. Two early Holocene rock avalanches in the Bernese Alps (Rinderhorn, Switzerland). *Geomorphol.*, 268:207-221.

GRUNER, U. 2006. Bergstürze und Klima in den Alpen-gibt es Zusammenhänge. *Bulletin für angewandte Geol.*, 11(2):25-34.

HANDY, R.L. & SPANGLER, M.G. 2007. *Geotechnical engineering: soil and foundation principles and practice*. New York: McGraw Hill.

HEIM, A. 1932. Bergsturz und Menschenleben. *Beibl. Vierteljahresschr. Naturforsch. Ges. Zürich*, 77(20):1-218.

HERMANN, R.L. 2013. Rock Avalanche (Sturzstrom). In: Bobrowsky, P.T. (ed.). *Encyclopedia of Natural Hazards*. Dordrecht: Springer 875-899.

HIGGS, K.E., HAESE, R.R., GOLDING, S.D., SCHACHT, U. & WATSON, M.N. 2015. The Pretty Hill Formation as a natural analogue for CO₂ storage: An investigation of mineralogical and isotopic changes associated with sandstones exposed to low, intermediate and high CO₂ concentrations over geological time. *Chem. Geol.*, 3992015/04/02/:36-64.

HJULSTRÖM, F.H. 1935. Studies of the morphological activity of rivers as illustrated by the river Fyris. *Bull. Geol. Ass. Uppsala*, 25:221-525.

HÖLTING, B. & COLDEWEY, W.G. 2013. *Hydrogeology: Introduction to General and Applied Hydrogeology*. Heidelberg: Springer.

HUTCHINSON, J.N. 1988. General report: Morphological and geotechnical parameters of landslides in relation to geology and hydrogeology. *Proceedings, 5th International Symposium on Landslides*, 1:3-35.

IMRE, B., LAUE, J. & SPRINGMAN, S.M. 2010. Fractal fragmentation of rocks within sturzstroms: insight derived from physical experiments within the ETH geotechnical drum centrifuge. *Gran. Matt.*, 12(3):267-285.

IVY-OCHS, S., HEUBERGER, H., KUBIK, P.W. & KERSCHNER, H. (1998). *The age of the Köfels event. Relative ¹⁴C and cosmogenic isotope dating of an early Holocene landslide in the central Alps (Tyrol, Austria)*. Unpublished manuscript, Innsbruck.

KASS, W. & BEHRENS, H. 1998. *Tracing technique in geohydrology*. Rotterdam: Balkema.

KÖRFGEN, A., MERGILI, M. & ZANGERL, C. 2014. GIS-based topographic reconstruction and geotechnical modelling of the Köfels Rockslide (Austria). *Geophys. Res. Abst.*, 16:6621.

LEGROS, F. 2002. The mobility of long-runout landslides. *Eng. Geol.*, 63(3):301-331.

LEUCHS, K. 1921. Die Ursachen des Bergsturzes am Reintalanger (Wettersteingebirge). *Geol. Rds.*, 12(3):189-192.

MATZNETTER, J. 1956. The process of mass movements using examples of the Klostertal in Vorarlberg. *Nat. Hazards Earth Syst. Sci.*(25):30.

MEILI, R., IMRE, B., LAUE, J., ASKARINEJAD, A. & SPRINGMAN, S.M. 2013. Die Toma Hügel des Fernpass Bergsturzes. In: Heißel, G., Mostler, W. (ed.). *Geoforum Umhausen*.16-19.

MOSTLER, W. 2013. Der Fernpassbergsturz in völlig neuem Lichte. *Geoforum Umhausen*, 15:20-28.

MURTHY, V.N.S. 2002. *Geotechnical engineering: principles and practices of soil mechanics and foundation engineering*. Florida, United States: CRC press.

NUSSBAUM, F. 1934. Ueber die Formen von Bergsturzmassen, mit besonderer Berücksichtigung des Bergsturzes im Kandertal. *Der Scheizer Geograph.*(11):12-13.

OSTERMANN, M., SANDERS, D., IVY-OCHS, S., ALFIMOV, V., ROCKENSCHAUB, M. & RÖMER, A. 2012. Early Holocene (8.6ka) rock avalanche deposits, Obernberg valley (Eastern Alps): Landform interpretation and kinematics of rapid mass movement. *Geomorphol.*, 171-172:83-93.

OSTERMANN, M., SANDERS, D., IVY-OCHS, S. & ROCKENSCHAUB, M. 2013. The rock avalanche in Obernberg valley (Tyrol, Austria): Characteristics and age. *Geophys. Res. Abst.*, 15:4941-4942.

PAGUICAN, E., DE VRIES, B.V.W. & LAGMAY, A. 2014. Hummocks: how they form and how they evolve in rockslide-debris avalanches. *Landslides*, 11(1):67-80.

PÁNEK, T. & KLIMEŠ, J. 2016. Temporal behaviour of deep-seated gravitational slope deformations: A review. *Earth-Sci. Reviews*, 156:14-38.

PEDRAZZINI, A., JABOVEDOFF, M., LOYE, A. & DERRON, M. 2013. From deep seated slope deformation to rock avalanche: Destabilization and transportation models of the Sierre landslide (Switzerland). *Tectonophysics*, 605:149-168.

PENCK, A. 1882. *Die Vergletscherung Der Deutschen Alpen*. Leipzig: Springer.

PENCK, A. & BRÜCKNER, E. 1901. *Die Alpen im Eiszeitalter*. Leipzig: Springer.

POLLET, N., SCHNEIDER, J.L., SCHMITTER-VOIRIN, C., WASSMER, P., CHAPRON, E. & WESSELS, M. 2000. Une tragédie alpine il y a 8000 ans: le sturzstrom de Flims (Grisons, Suisse) et ses conséquences cindyniques. *Colloque Géomorphologie et Risques Naturels, Lille(9)*:103-116.

POSCHINGER, A.V. & KIPPEL, T. 2009. Alluvial deposits liquefied by the Flims rock slide. *Geomorphol.*, 103:50-56.

POSCHINGER, A.V., WASSMER, P. & MAISCH, M. 2006. The Flims rockslide: history of interpretation and new insights. *Landslides from massive rock slope failure*, 49(5):329-356.

POULIQUEN, O., DELOUR, J. & SAVAGE, S.B. 1997. Fingering in granular flow. *Nature*, 386(6627):816-817.

PRAGER, C., IVY-OCHS, S., OSTERMANN, M., SYNAL, H.-A. & PATZELT, G. 2009a. Geology and radiometric ¹⁴C-, ³⁶Cl- and Th-/U-dating of the Fernpass rockslide (Tyrol, Austria). *Geomorphol.*, 103(1):93-103.

PRAGER, C., KRAINER, K., SEIDL, V. & CHWATAL, W. 2006a. Spatial features of Holocene Sturzstrom-deposits inferred from subsurface investigations (Fernpass rockslide, Tyrol, Austria). *Geo. Alp.*, 3:147-166.

PRAGER, C. & ZANGERL, C. 2005. Kinematics of a long run-out rockslide: a case study from the Fernpass-region (Northern Calcareous Alps, Tyrol, Austria). *Geophys. Res. Abstr.*:02737.

PRAGER, C., ZANGERL, C., BRANDNER, R., KRAINER, K. & CHWATAL, W. 2006b. Structure and kinematics of a long run-out rockslide: the Holocene Fernpass Sturzstrom (Northern Calcareous Alps, Tyrol, Austria). *Pangeo Austria*:259-261.

PRAGER, C., ZANGERL, C. & NAGLER, T. 2009b. Geological controls on slope deformations in the Köfels rockslide area (Tyrol, Austria). *Austrian Jour. Earth Sci.*, 102:4-19.

PRAGER, C., ZANGERL, C., PATZELT, G. & BRANDNER, R. 2008. Age distribution of fossil landslides in the Tyrol (Austria) and its surrounding areas. *Nat. Hazards Earth Syst. Sci.*, 8:377-407.

REISER, M.K., SCHEIBER, T., FÜGENSCHUH, B. & BURGER, U. 2010. Hydrogeological characterisation of lake Obernberg, Brenner Pass Area, Tyrol. *Austrian J. Earth Sci.*, 103(1).

SAM, L., BHARDWAJ, A., SINGH, S. & KUMAR, R. 2015. Remote sensing flow velocity of debris-covered glaciers using Landsat 8 data. *Progress in Phys. Geo.*:0309133315593894.

SANDERS, D., OSTERMANN, M., BRANDNER, R. & PRAGER, C. 2010. Meteoric lithification of catastrophic rockslide deposits: Diagenesis and significance. *Sedimentary Geol.*, 223(1):150-161.

SASSA, K., FUKUOKA, H., WANG, F. & WANG, G. 2007. *Progress in landslide science*. Heidelberg: Springer.

SCHMID, S.M., FUGENSHUH, B., KISSLING, E. & SCHUSTER, R. 2004. Tectonic map and overall architecture of the Alpine orogeny. *Eclogae geol. Helv.*, 97:93-117.

SCHNEIDER, J.L., WASSMER, P. & LEDÉSERT, B. 1999. La fabrique interne des dépôts du sturzstrom de Flims (Alpes suisses): caractéristique et implications sur les mécanismes de transport. *Comptes Rendus de l'Académie des Sciences, Sciences de la terre et des planètes, Paris*, 328:607-613.

SCHUCH, M.F. 1981. Bericht über die Ergebnisse der Hydrogeologischen Untersuchungen im Bereiche des Weißen-, Mitter- u. Finstersees. Michael F. Schuch, Innsbruck, 14.

SERERHARD, N. 1872. *Einfahte Delineation aller Gemeinden gemeiner dreien Bünden nach der Ordnung der hochgerichten eines jeden Bunds, ihren Nammen, Nachbarschafften, Höfen, Situationen, Landsart, Religion und Land-Sprach nach kurz entworfen samt beigefügten etweschen Merkwürdigkeiten der Natur... vom Jahre 1742*. Verlag der Antiquariatsbuchhandlung.

SHEA, T. & DE VRIES, B.V. 2008. Structural analysis and analogue modeling of the kinematics and dynamics of rockslide avalanches. *Geosphere*, 4(4):657-686.

SMELLIE, J.A.T., KARLSSON, F. & ALEXANDER, W.R. 1997. Natural analogue studies: present status and performance assessment implications. *J. Contam. Hydrol.*, 26(1):3-17.

STAUB, W. 1910. *Die Tomalandschaften im Rheintal von Reichenau bis Chur: ein Beitrag zur Kenntnis der Bergsturzablagerungen im Rheintal*. Switzerland: Haller'sche Buchdruckerei.

SUNDBORG, Å. 1956. The River Klaralven: a study of fluvial processes. *Geografiska Annaler*, 38(3):238-316.

TÓTH, J. 1963. A theoretical analysis of groundwater flow in small drainage basins. *J. Geophys. Res.*(68):4795-4812.

VALDERRAMA, P., ROCHE, O., SAMANIEGO, P., DES VRIES, B.V. & ARAUJO, G. 2018. Granular fingering as a mechanism for ridge formation in debris avalanche deposits: Laboratory experiments and implications for Tutupaca volcano, Peru. *J. Volcanol. Geoth. Res.*, 349:409-418.

VAZQUEZ BORRAGAN, A. 2014. Modelling Internal Erosion Within An Embankment Dam Prior To Breaching. Stockholm, Royal Institute of Technology.

VON POSCHINGER, A. 2011. The Flims rockslide dam. In: Evans S., H.R., Strom A., Scarascia-Mugnozza G. (ed.). *Natural and Artificial Rockslide Dams*. Heidelberg: Springer: 407-421.

WASSMER, P., SCHNEIDER, J.L., POLLET, N. & SCHMITTER-VOIRIN, C. 2004. Effects of the internal structure of a rock avalanche dam on the drainage mechanism of its impoundment, Flims sturzstrom and ilanz paleo-lake, Swiss Alps. *Geomorphol.*, 61:3-17.

WOLKERSDORFER, C. 1991. Anfschluß an einem Tomahügel des Fernpaßbergsturzes/Tirol. *Jb. geol. B.-A.*, 134(2):439-441.

WOLKERSDORFER, C. 2008. *Water management at abandoned flooded underground mines: fundamentals, tracer tests, modelling, water treatment*. Heidelberg: Springer.

WOLKERSDORFER, C., MORE, K. & LUPANKWA, M. 2017. Analoge Modellierung von Tomahügeln [An analogue Toma Hill Model], In: Heißel, G., Mostler, W. (Eds.), *Geoforum Umhausen, Umhausen*, pp. 61-69.